Delineating the extra-virgin olive oil aroma blueprint by multiple headspace solid phase microextraction and differential-flow modulated comprehensive two-dimensional gas chromatography

Delineating the extra-virgin olive oil aroma blueprint by multiple headspace solid phase microextraction and differential-flow modulated comprehensive two-dimensional gas chromatography

Federico Stilo[1], Maria del Pilar Segura Borrego[2], Carlo Bicchi[1], Sonia Battaglino[1], Raquel Maria Callejón Fernadez[2], Maria Lourdes Morales[2], Stephen E. Reichenbach[3,4], James Mc Curry[5], Daniela Peroni[6], Chiara Cordero[1]*

Authors' affiliation:

1. University of Turin, Dipartimento di Scienza e Tecnologia del Farmaco, Turin, Italy
2. Área de Nutrición y Bromatología, Dpto. de Nutrición y Bromatología, Toxicología y Medicina Legal, Facultad de Farmacia, Universidad de Sevilla, Sevilla, Spain
3. Computer Science and Engineering Department, University of Nebraska – Lincoln, Lincoln, NE, USA
4. GC Image LLC, Lincoln, NE, USA
5. Agilent Technologies, Gas Phase Separations Division, Wilmington DE, USA
6. SRA Intruments SpA, Cernusco sul Naviglio, Milan, Italy

*Corresponding author:

Dr. Chiara Cordero - Dipartimento di Scienza e Tecnologia del Farmaco, Università di Torino, Via Pietro Giuria 9, I-10125 Torino, Italy – e-mail: chiara.cordero@unito.it; phone: +39 011 6707172

Abstract

Comprehensive two-dimensional gas chromatography with parallel mass spectrometry and flame ionization detection (GC×GC-MS/FID) enables effective chromatographic fingerprinting of complex samples by comprehensively mapping untargeted and targeted components. Moreover, the complementary characteristics of MS and FID open the possibility of performing multi-target quantitative profiling with great accuracy. If this synergy is applied to the complex volatile fraction of food, sample preparation is crucial and requires appropriate methodologies capable of providing true quantitative results.

In this study, untargeted/targeted (*UT*) fingerprinting of extra-virgin olive oil volatile fractions is combined with accurate quantitative profiling by multiple headspace solid phase microextraction (MHS-SPME). External calibration on fifteen pre-selected analytes and FID predicted relative response factors (RRFs) enable the accurate quantification of forty-two analytes in total, including key-aroma compounds, potent odorants, and olive oil geographical markers.

Results confirm good performances of comprehensive UT fingerprinting in developing classification models for geographical origin discrimination, while quantification by MHS-SPME provides accurate results and guarantees data referability and results transferability over years. Moreover, by this approach the extent of internal standardization procedure inaccuracy , largely adopted in food volatiles profiling, is measured. Internal standardization yielded an average relative error of 208 % for the fifteen calibrated compounds, with an overestimation of + 538% for (*E*)-2-hexenal, the most abundant yet informative volatile of olive oil, and a -89% and -80% for (*E*)-2-octenal and (*E*)-2-nonenal respectively, analytes with a lower HS distribution constant.

Compared to existing methods based on 1D-GC, the current procedure offers better separation power and chromatographic resolution that greatly improve method specificity and selectivity and results in lower LODs and LOQs, high calibration performances (*i.e.*, R^2 and residual distribution), and wider linear range of responses.

As an *artificial intelligence smelling machine*, the MHS-SPME-GC×GC-MS/FID method is here adopted to delineate extra-virgin olive oil aroma blueprints; an objective tool with great flexibility and reliability that can improve the quality and information power of each analytical run.

Keywords:

Extra-virgin olive oil volatiles; comprehensive two-dimensional gas chromatography; parallel detection MS/FID; predicted relative response factors; reverse-inject differential-flow modulation; quantitative analysis

1. Introduction

Comprehensive two-dimensional gas chromatography (GC×GC) coupled to mass spectrometry (MS), by combining physico-chemical discrimination of sample constituents with spectrometric diagnostic signatures, provides qualitative and quantitative information about single analytes and/or groups of analytes and is the basis for in-depth comprehensive investigations with fingerprinting and profiling [1–3]. The improved separation power of GC×GC, compared to one-dimensional (1D) GC, accompanied by logical retention patterns for chemically related compounds and specialized data processing techniques, make GC×GC-MS one of the most suitable platforms for accurate and informative investigations on complex samples. Moreover, GC×GC-MS performance, information dimensions, and flexibility are crucial to achieve reliable and consistent results when the analytical process is used to answer many different questions about functional variables related to a sample's chemical composition [1,4].

When the fraction under study poses challenges because of the large dynamic range of concentrations covered and consists of analytes with a wide polarity range within a relatively narrow volatility interval, chromatographic resolution and efficiency are fundamental to achieve appropriate method performances. The role of sample preparation, as the zeroth dimension of the system and as a key step of the analytical method, is crucial and its design/set-up requires careful consideration of the analysis' final goal(s). If a targeted profiling of selected components is the goal, sample preparation efforts can be directed to known analytes and performance parameters optimized to achieve high specificity and selectivity, appropriate repeatability, and accuracy for those selected targets. However, if the aim of the investigation is untargeted fingerprinting of all detectable constituents, then sample preparation must be comprehensive and minimally analytes/class-specific, in order to limit discriminations and improve the breadth of the analysis [1]. Moreover, sample preparation should be able to exploit a large dynamic range of analytes' concentrations while providing solid foundations for quantitative cross-comparisons.

In the context of complex volatile fractions of food origin, GC×GC-MS has been demonstrated to be very effective for both untargeted and targeted investigations (e.g., combined untargeted/targeted fingerprinting approaches [5,6]) by combining high-throughput fingerprinting with quantitative profiling [7] in the same analysis. In these applications, the role of headspace (HS) solid-phase microextraction (SPME) as the sampling approach, is central, and its main limits, related to the actual volume/amount of extracting/accumulating phase, are fully compensated by the analytical performances of GC×GC.

In this study, we make a step forward in the exploitation of the HS-SPME-GC×GC-MS potentials by designing a procedure capable of performing comprehensive chromatographic fingerprinting of the complex volatile fraction of high-quality extra-virgin olive oil (EVOO) while providing accurate quantitative data on a large list of targeted analytes (*i.e.*, targeted quantitative profiling [1]) with a high informative potential related to samples' sensory quality and qualification. Moreover, the procedure is highly automated, limiting manual operations to a few simple

steps, and implemented on a robust, reliable, and commercially available analytical platform in order to be considered suitable for high-throughput screenings and quality control assessments. The differential-flow modulation technology was chosen as a core element of the GC×GC platform. Its stable performance and relative ease of use [8–13], accompanied by the possibility of rationally translating validated methods from thermal modulated systems [8,14,15], are key-aspects to design a method complying with minimal performance requirements in EU quality standards for analytical measurements [16,17].

Mediterranean countries offer ideal conditions for olive tree (*Olea europaea* L.) cultivation [18] and have preserved and valorized olive oil (OO) manufacturing traditions including harvest methodologies and milling technologies [19,20]. High-quality OOs, complying with EU Regulations and International Standards for production, chemical composition, and sensory quality, are labelled as *extra-virgin* (EV)OOs (EEC No 2568/91 and its amendments; IOC/T.20/Doc. No 15/Rev. 10 2018). Within EVOOs, due to peculiar characteristics of olive cultivar(s), pedo-climatic conditions of the harvest region, and traditions related to milling technology, the EU recognizes additional qualities through quality schemes and labels. The Protected Designation of Origin (PDO) products, for example, are those which "*have the strongest links to the place in which they are made*" and "*every part of the production, processing and preparation process must take place in the specific region*" [21].

In this context, the possibility to accurately map high-quality EVOO volatiles (i.e., volatiles fingerprinting) with additional information about the concentrations/amounts of informative components, represents a step forward in the rationalization of the quality concept. To date, EVOO quality is defined by its compliance with physicochemical indices (e.g., free acidity, peroxide index, UV absorbance) and by absence of sensory defects and presence of a perceivable *fruity* attribute (*i.e.*, median M>0). Nevertheless, these standards do not provide elements for valorization and discrimination of products with superior sensory quality or obtained within PDO and Protected Geographical Indication (PGI) recognized protocols. A methodology, capable of generating a sample's fingerprint with identitation potentials [22] accompanied by the accurate quantification of selected chemical markers, might fill this gap while improving the knowledge on EVOO quality signatures, its *aroma blueprint* [23,24], and its unicity across production regions and harvest years.

Within EU quality standards for analytical methodologies, specificity and selectivity are matched by a suitable combination of separation phase chemistries in the two chromatographic dimensions; sensitivity is achieved by careful tuning the columns combination dimensions (first dimension – ^{1}D and second dimension – ^{2}D lengths and diameters) and differential flows; identity confirmation is achieved by MS spectral signature matching constrained by two retention time points ($^{1}t_R$ and $^{2}t_R$); and quantitative accuracy is achieved by external calibration and data cross-validation with two parallel detectors (*i.e.*, MS and flame ionization detector FID). Parallel detection

by MS/FID, extends the method's linear range over two-to-three orders of magnitude of actual analytes' concentrations [25], and opens the possibility of adopting reliable response factors for quantitative estimations [10,26].

To achieve accurate quantitative results, the multiple headspace extraction (MHE) approach is combined with the enrichment capacity of SPME with a multi-component fiber (*i.e.*, divinylbenzene/carboxen/polydimethyl siloxane) extensively adopted in EVOO volatiles' profiling [27,28]. The challenging aspect of the MHS-SPME procedure consists in the need of avoiding headspace saturation, the basis of quantification inaccuracy of many methods, while enabling multi-analyte quantification even without external calibration.

This study adds a further, advanced, and extremely flexible tool for quality control and valorization of high-quality EVOOs, acting as a bridge between 1D-GC based methods for fingerprinting [29] and/or quantitative profiling of selected key-markers [27,30] to advanced high-information methods based on GC×GC technology [5,24,31,32]. Methods performances are tested over a set of fifty EVOO samples from Italian top-quality production [33,34], obtained from different olives cultivars and from three harvest areas. Fingerprinting potentials are explored briefly and then compared to the targeted quantitative profiling information power. Quantification accuracy is demonstrated over a set of fifteen informative chemicals subjected to external quantification by MHS-SPME and toward an extended set including forty-two volatiles for which predicted FID relative response factors (RRFs) can be applied. Results are critically compared to existing methods based on 1D-GC-FID or 1D-GC-MS, and the advantages derived from improved information potential are discussed in the perspective of an objective qualification of high-quality products, including their sensory features, by reliable and standardized instrumental methods.

2. Materials and methods

2.1 Reference standards and solvents

Pure standards of *n*-alkanes (from *n*-C9 to *n*-C25) used for Linear Retention Indices (I^T) calibration, of α/β-thujone and 2-methyloctynoate used as Internal Standards (ISTDs), and solvents (cyclohexane and dibutyl phthalate – 99% of purity) were from Merck (Milan, Italy).

The following key-aroma compounds and potent odorants, selected according to reference literature [35–41] and adopted for external calibration, were from Sigma Aldrich (Milan, Italy): (*E*)-2-pentenal (CAS 1576-87-0), (*E*)-2-penten-1-ol (CAS 1576-96-1), (*Z*)-2-penten-1-ol (CAS 1576-95-0), 1-penten-3-ol (CAS 616-25-1), 1-pentanol (CAS 71-41-0), 2-pentanol (CAS 6032-29-7), ethyl acetate (CAS 141-78-6), (*E,E*)-2,4-hexadienal (CAS 142-83-6), (*E*)-2-hexenal (CAS 6728-26-3), (*Z*)-3-hexen-1-ol (CAS 928-96-1), hexanal (CAS 66-25-1), 1-hexanol (CAS 111-27-3), heptanal (CAS 111-70-6), (*E*)-2-octenal (CAS 2548-87-0), and (*E*)-2-nonenal (CAS 18829-56-6).

2.2 Reference solutions and calibration mixtures

Standard stock solutions of reference analytes were prepared at a concentration of 10 g/L in cyclohexane and stored at -18°C for one-week.

The Reference Working Solution (RWS) was prepared by mixing suitable amounts of standard stock solutions to reach the concentration of 0.250 g/L using dibutyl phthalate as solvent.

Calibration solutions (CS) were prepared by diluting suitable amounts of RWS in dibutyl phthalate to reach the final concentrations: 30, 25, 20, 15, 10, 5, 2, 1, 0.5, 0.2 mg/L. Calibration curves were built by analyzing 5 µL of each CS by MHS-SPME while matching absolute amounts of 150, 125, 100, 100, 75, 50, 25, 10, 5, 2.5, 1 ng.

ISTDs working solution for standard-in fiber pre-loading [42] was prepared at 0.100 g/L in dibutyl phthalate and stored at -18°C in sealed vials.

A schematic diagram of the operative procedure is reported in the Supplementary material.

2.3 Extra virgin olive oil samples

EVOO samples were collected within the VIOLIN project (Valorization of Italian OLive products through INnovative analytical tools) [34]. They were obtained from olives of different cultivars harvested in 2017 over the Italian territory. Details on the sample-set under study are provided in Table 1 together with harvest regions (*i.e.*, *Sicilia*, *Toscana,* and *Garda* lake) shown in Supplementary Figure 1.

2.4 Multiple headspace solid phase microextraction: devices and conditions

Volatiles from EVOO samples were extracted by HS-SPME with a divinylbenzene/carboxen/polydimethyl siloxane (DVB/CAR/PDMS) fiber (d_f 50/30 µm; 2 cm length) from Supelco (Bellefonte, PA, USA) chosen based on literature on sampling effectiveness for EVOO's informative compounds [24,32,37,43]. The SPME fiber was conditioned before use as recommended by the manufacturer.

The ISTDs for response normalization and quality control were preloaded onto the SPME device [42,44] by sampling 5.0 µL of α/β-thujone and methyl 2-octynoate ISs solution (0.100 g/L) placed in a 20 mL headspace vial. ISTDs pre-loading was performed by exposing the SPME device in the HS at a temperature of 40 °C for 5 min.

Sampling was carried out on 0.100 ± 0.005 g of oil, precisely weighed, in 20 mL headspace vials, kept at 40°C for 60 minutes under constant agitation. The very low amount of sample was chosen to match HS linearity conditions for most of the characteristic analytes of the EVOO volatilome [37,45]. After extraction, the SPME device was automatically transferred to the split/splitless injection port of the GC×GC system, kept at 250 °C, and thermal desorption was for 5 min. Samples were analyzed in three replicates randomly distributed over a two-week time frame.

MHS-SPME from samples and calibration solutions was conducted by applying the above indicated conditions, and the number of consecutive extraction steps was set to five, achieving an almost exhaustive extraction for the analytes under study [46].

2.5 GC×GC-MS/FID with reverse-inject differential flow modulation: instrument set-up and conditions

Automated MHS-SPME, as described in *Section 2.4*, was performed by a multipurpose sampler, model MPS-2 (Gerstel, Mülheim a/d Ruhr, Germany), installed on a GC×GC system equipped with a reverse-inject differential-flow modulator based on capillary flow technology™ (Agilent Technologies, Little Falls, DE, USA). The Agilent 7890B GC unit was coupled to an Agilent 5977B HES (high efficiency source) fast quadrupole MS detector (Agilent Technologies, Little Falls, DE, USA) operating in electron ionization mode at 70 eV. Ion source and transfer-line temperatures were set at 280 °C, and the quadrupole temperature was set at 240°C. The scan range was set between 45 and 240 *m/z*, achieving an actual data acquisition frequency of 30 Hz. Parallel detection was by a fast FID with base temperature 280 °C; H_2 flow 40 mL/min, air flow 350 mL/min, and sampling frequency 200 Hz.

The column set was configured as: ^{1}D HeavyWax™ column (100% polyethylene glycol - PEG; 20 m × 0.18 mm *dc* × 0.18 µm *df*) coupled with ^{2}D DB17 column (50% phenyl-methylpolysiloxane; 1.8 m × 0.18 mm *dc* × 0.18 µm *df*), both from Agilent Technologies (Wilmington, DE, USA). The connection between the ^{2}D column and deactivated silica capillaries (Agilent Technologies) toward MS (0.5 m × 0.1 mm *dc*) and FID (1.1 m x 0.18 mm *dc*) for parallel detection was by a three-way unpurged capillary microfluidic splitter (G3181B, Agilent, Little Falls, DE, USA). The resulting split ratio was 70:30 FID/MS. The bleeding capillary of deactivated fused silica (6.06 m × 0.1 mm *dc*) installed on the modulator plate was dimensioned according to a previously validated flow calculator [15].

The GC split/splitless injector port was set at 250 °C and operated in pulsed-split mode (250 kPa overpressure applied to the injection port until 2 min) with a split ratio 1:20. A special design liner for SPME thermal-desorption (Merck) was used to improve analytes transfer into the ^{1}D column and limit band broadening in space. The carrier gas was helium at a nominal flow of 0.4 mL/min along the ^{1}D column and 10 mL/min along the ^{2}D column. The oven temperature program was set as: from 40 °C (2.29 min) to 240°C (11') at 3.06 °C/min and determined by method translation of a reference method previously validated in the authors' laboratory [10,32]. The modulation period (P_M) was set at 3s and pulse time at 150 ms.

The *n*-alkanes liquid sample solution for I^T determination was analyzed under the following conditions: split/splitless injector in split mode, split ratio 1:50, injector temperature 250 °C, and injection volume 1 µL.

2.6 External standard calibration by MHS-SPME-GC×GC-MS/FID

Calibration curves were built to cover analyte absolute amounts in the analyzed samples within the range 1-150 ng. External standard calibration was conducted on both MS and FID traces. For the MS detection channel, extracted target ions (Ti) were selected for each analyte; *m/z* values are reported in Table 2. Up to three additional qualifier ions (Q1, Q2, Q3) were also monitored for quality evaluation. For the FID channel, external calibration was based on 2D peak volumes; analytes affected by coelution issues were only quantified by MS. Additional details on the calibration/quantification procedure are discussed in *Section 3.2*.

Table 2 lists target analytes subjected to external calibration together with their odor quality, odor threshold (OT), experimental I^T, Ti and Qs *m/z*, regression functions parameters including calibration range, determination coefficients (R^2), and precision.

2.7 Data acquisition and 2D data processing

Data were acquired by Enhanced MassHunter (Agilent Technologies, Little Falls, DE, USA) and processed by GC Image® suite, Release 2.9 (GC Image, LLC, Lincoln NE, USA). Statistical analysis and chemometrics were by XLSTAT statistical and data analysis solution software (Addinsoft 2020, New York, USA).

3. Results and discussion

3.1 The information potential of olive oil volatiles patterns

EVOO volatile fractions are complex mixtures of compounds belonging to different chemical classes (*e.g.*, aldehydes, ketones, alcohols, esters, lactones, hydrocarbons, terpenes), whose relative distributions reflect concurrent functional variables strongly correlated to relevant quality concepts: cultivar, geographical origin, quality (*i.e.,* EVOO, virgin olive oil – VOO, and lampante olive oil – LOO), olive ripeness, technological processes, and storage conditions [24]. Within this complex fraction, potent odorants are those components that, reaching the olfactory epithelium, dissolve into the mucus and interact with olfactory receptors, triggering olfaction and modulating the final aroma perception [36]. Potent odorants in their natural concentration in food define the odor code or aroma blueprint [23] and are at the basis of a rational sensory coding process, recently defined as "artificial intelligence smelling", of great interest for food industry and market [47].

In this study, chromatographic fingerprinting was based on the combined untargeted/targeted (UT) fingerprinting process [5,32,45] while accurate quantification was primarily directed to a selection of impacting odorants defining high-quality EVOO aroma. Contributing to *fresh-green* and *fruity* notes, positive attributes [20] in EVOOs, are C5 and C6 oxygenated compounds (*i.e.*, alcohols and carbonyls). In particular, (*E*)-2-pentenal, (*Z*)-2-penten-1-ol, 1-penten-3-ol, 1-pentanol, (*E,E*)-2,4-hexadienal, (*E*)-2-hexenal, (*Z*)-3-hexen-1-ol, hexanal, and 1-hexanol were targeted and subjected to quantitative profiling by external standard calibration. They belong to the so-called lipoxygenase (LOX) signature [36–40] and are formed by enzymatic oxidation of linolenic and linoleic acids through the LOX pathway [40].

Compounds responsible for sensorial defects also were included, although they were expected to be at very low concentrations, if not below the method's limit of detection (LOD), due to the quality level and freshness of selected samples. This group included some C_7-C_{10} linear saturated and unsaturated aldehydes deriving from fatty acids hydroperoxides cleavage: heptanal, (*E*)-2-octenal, and (*E*)-2-nonenal. They provide information on the autoxidation process and shelf-life evolution, and their increasing concentration is correlated to the perception of *rancid* and *fatty* notes [35,37,38].

The targeted compounds list was completed by analytes correlated to well-known sensory defects [36,38,39]: (*E*)-2-penten-1-ol, with *mushroom-like* and *earthy* sensations; 2-pentanol, related to *musty* and *fermented* perception; and ethyl acetate, responsible for the *winey* note [36,38,39]. **Table 2** lists targeted analytes together with their odor quality, odor threshold (OT) in oil as reported in literature, experimentally determined I^T, and additional information related to the quantification procedure. Details are discussed in the next sections.

Figure 1 shows pseudocolor images of volatile patterns from an EVOO sample analyzed by a polar × semi-polar column combination (*i.e.*, PEG × OV1701) and resulting from the parallel detection by MS (**Figure 1A**) and FID

(Figure 1B). Enlarged areas of the chromatographic plane highlight the complexity of the patterns, the chromatographic resolution of analyte clusters obtained by combining the two separation dimensions, and the wide range of response variations (perceivable by colorization) spanned by detected volatiles in the two detection channels. The list of targeted analytes, including those that were not subjected to quantitative assessment, is provided in Supplementary Table 1, together with their retention times in the two chromatographic dimensions (^1t_R - min, ^2t_R - sec), experimental I^T, odor descriptor, and OT (ng/g). Supplementary Table 2 lists untargeted and targeted peak features, identified by unique labelling on both detection channels (*i.e.*, #ID and chemical names), together with retention times in the two chromatographic dimensions (^1t_R - min, ^2t_R - sec), experimental I^T, and raw MS spectra.

3.*2 Accuracy of multiple headspace extraction vs. internal standardization for selected potent odorants*

Quantitative analysis is one of the most challenging aspects related with HS sampling, especially when carried out through high concentration capacity techniques based on accumulating polymers/materials, as for SPME. The main issues related to erroneous results are standardization and/or normalization of accumulating polymer(s) performance(s) and accuracy of the selected quantification approach [48].

Among the most common approaches, those based on internal standard(s) (ISs) require careful consideration about the quality of information that they provide. ISs methods are fast and simple and take into account and compensates for detector response variations and sampling variability when applied to liquid samples/extracts, but cannot be considered accurate [17] if analytes subjected to quantification have different HS partition constants (K_{HS}) and accumulating polymer/material distribution constants (K_D) under the applied sampling conditions. Moreover, when MS is adopted, the differential fragmentation rate and/or relative response of selected *Ti* might add further quantification errors related to the specific response factor of the analytes *vs*. that of ISs [49].

To overcome inaccuracy issues related to the lack of an appropriate modelling of the actual phenomena occurring in the HS sampling, external calibration is compulsory, although in the case of HS methods, the matrix effect would require its implementation in the form of standard addition (SA) procedure [50]. Moreover, SA provides accurate results if HS sampling operates in equilibrium conditions and/or if analytes HS saturation does not occur [37,45,50,51].

To achieve accurate quantification of multiple volatile targets in a single run, by operating in a wide dynamic range of analytes concentration, adopting non-equilibrium sampling with high efficient yet standard multi-component SPME devices, MHE method is the elective route [49,52]. MHE was introduced by Suzuki *et al.* [53] and McAuliffe [54] for static HS sampling to measure the total amount of the target analyte in the investigated matrix. It was further developed and modeled by Kolb and Ettre [52] and then successfully extended to HS-SPME sampling [48,50,55–58]. Principles of operation and fundamental equations are well detailed in reference literature

[48,50,55–58] and briefly summarized in the **Supplementary material**.

Table 2 reports, for the fifteen target odorants, information about calibration ranges (expressed in ng, as absolute amount of analyte in the HS), calibration functions for MS and FID channels accompanied by determination coefficients (R^2), and intermediate precision expressed as the characteristic % relative standard deviation (RSD%) obtained by replicated quantitative measurements of a representative sample over two-weeks. *(E)*-2-pentenal, 1-pentanol, ethyl acetate, *(E)*-2-hexenal, hexanal, and 1-hexanol required a two-step calibration to match for linearity on MS channel. Limit of detection (LOD) and limit of quantitation (LOD) also are reported for the FID channel. They were estimated according to EU protocol for food safety analytical methods performance parameters [59] by extrapolation from calibration curves.

Due to the lack of certified reference materials (CRM), quantification accuracy was defined through recovery % and precision [17]. Recovery was determined by multiple extraction (until exhaustive extraction) of CSs (i.e., blank matrix spiked with known amounts of target analytes) and of selected oil samples; quantification error (i.e., inaccuracy or bias) was then expressed as % relative error (%RE). Moreover, recovery data were validated by internal cross-matching between MS and FID values. Results on accuracy are visualized with histograms in **Figure 2A** with dark blue and orange bars accompanied by imprecision intervals. Amounts correspond to the average values of replicated analyses (n=3) of the 25 ng CS experiment. Expected values (*i.e.*, 25 ng) are marked with a green line while boundary, the light green bar, highlights a ± 20% error tolerance [17].

Of relevance are results on quantification error occurring by applying the ISs approach (see **Equation 1** in **Supplementary material**) with a relative response factor RFF=1 (light blue and orange bars in Figure 2A)..

The MHS-SPME method results can be considered accurate according to EU quality standards for analytical methods [17]; this is true for both MS and FID channels, respectively dark blue and orange bars in **Figure 2A**. Almost all analytes were quantified with a %RE less than 20. For the MS channel, the error is 11.7% with a maximum of 25.8% for (*E*)-2-nonenal, whereas for the FID, it achieves 9.5% with a maximum of 21.1% resulting from the quantification of (*E*)-2-pentenal. %RE increases up to 80 when the IS method is applied. In particular, for the MS detection channel, the %RE is 35.6, with eleven of fifteen compounds quantified having an error greater than 20% and a maximum value of 79.3% for 1-penten-3-ol. Accuracy was slightly better for the FID channel with an average error of 21.1%, with eight of fifteen compounds quantified with %RE greater than 20 and a maximum of 47.7 for quantification of (*E*)-2-nonenal.

Of interest are quantification results estimated on the test sample (*i.e.*, EVOO S1 from *Sicilia*) and shown in histogram of **Figure 2B.** Here the %RE between the MHS-SPME approach (taken as reference for comparison) and HS-SPME quantification based on the IS was calculated for the FID channel. The average %RE for the IS approach was 208% with a maximum of +538% for (*E*)-2-hexenal. This analyte is the most abundant in the EVOO volatile

fraction and is highly informative, being a key-aroma compound validated by sensomics [35]. Its overestimation might lead to erroneous conclusions about a sample's aroma blueprint. Similar results were obtained for other highly abundant components, such as 1-penten-3-ol, hexanal, (Z)-3-hexen-1-ol, and 1-hexanol, all characterized by steeper decay curves, *i.e.*, lower β values (further details are commented below.)

On the other hand, for compounds present in lower amounts and characterized by relatively flat decay curves and higher β values, as in the case of (*E*)-2-octenal and (*E*)-2-nonenal, underestimation was respectively -89% and -80%. Supplementary Table 3 reports accuracy (i.e, recovery and precision) results for analytes subjected to external calibration by MHS-SPME on selected CSs(1-10-25-100 ng) and on test samples S1, S8, T3, T10, G6, and G12, where exhaustive extractions were conducted until LOD.

These results evidence how inaccurate might be quantification that approximates detector relative response factors to unity (*i.e.*, by using a single IS for quantification) and does not consider analytes' specific K_{HS} and K_D under the applied conditions. Moreover, the adoption of non-equilibrium HS sampling – at least not for all targeted analytes – and the multi component characteristics of the SPME device (e.g., combining adsorption and absorption mechanisms) add further variables that make complex and challenging EVOO volatiles quantification.

3.3 Extending quantification to non-calibrated analytes by adopting FID predicted relative response factors

EVOO volatile fractions are highly-complex and the presence of a large number of informative components requires greater efforts to extend external calibrations to all analytes matching with HS linearity in the defined conditions. However, the possibility to extend the quantification potential of the analytical method to a large set of volatiles while keeping an appropriate accuracy is attractive. If achieved, batch-to-batch data transferability is possible, even for long-time frame studies and for different GC(×GC) technologies.

With parallel MS and FID detection, additional options for reliable quantification are available. In particular, while MS detection achieves high specificity by selecting specific ion traces in cases of co-elution and/or the presence of interferents [60], FID provides stable structure-specific response factors in a wider range of concentrations [51,61].

The adopted platform, combining high-resolution and efficient separation of analytes by GC×GC with parallel detection by MS/FID, opens the possibility of adopting FID predicted RRFs based on combustion enthalpies and molecular structure [61]. The alignment of the separation patterns from MS and FID detection, as illustrated in Figure 1, enables reliable analyte identification using multiple criteria (retention in two dimensions and MS spectral signature) and across the parallel channels, while quantification can be extended over uncalibrated compounds by estimating their FID RRFs with Equation 1.

Equation 1. $$\mathrm{RRF} = 10^3 * \left(\frac{MW_i}{MW_{IS}}\right) * (-61.3 + 88.8\eta_C + 18.7\eta_H - 41.3\eta_O + 6.4\eta_N + 64.0\eta_S - 20.2\eta_F - 23.5\eta_{Cl} - 10.2\eta_{Br} - 1.75\eta_I + 127\eta_{benz})^{-1}$$

where η_C, η_H, η_O, η_N, η_S, η_F, η_{Cl}, η_{Br}, η_I, and η_{benz} correspond to the number of carbon, hydrogen, oxygen, nitrogen, sulfur, fluorine, chlorine, bromine, and iodine atoms, and the number of benzene rings; and MW_i and MW_{IS} are the molecular weights of the analyte *i* and the *IS* adopted for the development of the model by de Saint Laumer *et al.* [61]. In this study, quantification was obtained from the peak area of each component normalized versus α-thujone as IS and corrected with its RRF calculated with Eq.1 to align combustion enthalpies normalized versus 1-hexanol here considered as internal reference. The analyte-specific RRF was corrected to the 1-hexanol/methyl octanoate ratio (i.e. $RRF_{i,1\text{-hexanol}} = 0.933/RRF_{i,\text{ methyl octanoate}}$) to adapt the model to 1-hexanol.

With predicted RRFs, quantitative profiling was extended to additional potent odorants, characterizing both positive attributes and specific sensorial defects, and to phenotypic markers. **Table 3** reports the RRF values calculated for targeted/calibrated analytes and for additional compounds of interest selected among those listed in **Supplementary Table 1**. They are: 3-pentanone, 1-penten-3-one, α-pinene, camphene, β-pinene, δ-3-carene, limonene, eucalyptol, hexyl acetate, octanal, *(Z)*-3-hexenyl acetate, *(E)*-2-heptenal, 6-methyl-5-hepten-2-one, nonanal, *(E)*-2-hexen-1-ol, acetic acid, *(E,E)*-2,4-heptadienal, α-copaene, benzaldehyde, propanoic acid, 1-octanol, butanoic acid, butyrolactone, y-hexalactone, propanal, (*Z*)-3-hexenal, and α-farnesene.

The list includes additional compounds formed along the LOX pathway and correlated to *green* and *fruity* notes: C5 ketones (*i.e.*, 3-pentanone and 1-penten-3-one), C6 esters (*i.e.*, hexyl acetate, (*Z*)-3-hexenal, and *(Z)*-3-hexenyl acetate), and C6 alcohols (*i.e.*, *(E)*-2-hexen-1-ol) [24,38,62–64].

Limonene, α-pinene, β-pinene, camphene, δ-3-carene, eucalyptol, α-copaene, and α-farnesene are terpenoids mainly known to be genetic and/or geographic markers [65]; nevertheless, they are odor active and could be associated with the perception of *herbal*, *pine,* and *citrus-like* notes [64,66]. 6-Methyl-5-hepten-2-one is a ripening indicator with *fruity-like* odor and propanal is present in high-quality EVOOs and described as *fresh, fruity* and *malty* [35,45,67,68].

Compounds related to sensorial defects include butyrolactone and y-hexalactone, described as contributing to the definition of the undesirable *oily* aroma [63]; acetic acid, propanoic acid, and butanoic acid, associated with *vinegary*, *musty* and *rancid* defects [38,62]; 1-octanol, usually found in oxidized samples [19,39] and with a *mushroom-like* odor; and benzaldehyde, whose presence is related to *moldy* and *earthy* defects [38]. Finally, octanal, nonanal, *(E)*-2-heptenal, and *(E,E)*-2,4-heptadienal contribute to *rancid* and *fatty* sensations.

Quantification results for the 42 targeted compounds are reported in **Supplementary Table 4**. The information they bring to the sample discrimination is considered in the next section. Italian EVOOs aroma blueprint is defined by considering key-aroma compounds concentration over the odor detection threshold (*i.e.*, odor activity value OAV).

3.4 Differential information encrypted in volatiles patterns: response vs. quantitative data

Volatiles fingerprints captured by mapping the responses of both untargeted and targeted features and 2D pattern information deriving from selected target volatiles bring differential information. The regional influence on the volatiles fraction, for example, can be examined by supervised chemometrics. Partial least square discriminant analysis (PLS-DA) was adopted to develop classification models based on the production region. Results are greatly illustrative on the information encrypted on global fingerprint and/or on 2D patterns with selected targets.

Figure 3A shows the score plot resulting from the PLS-DA model based on the global fingerprint information (i.e., *UT* fingerprinting process) and a cross-validation by *leave-n-out* approach (CV=4). The model was developed on the entire sample set (n=50) and resulted in an average sensitivity of 92.9% and a specificity of 97.4%. In particular, higher sensitivity was obtained for *Sicilia* EVOOs (100%) and lower sensitivity for *Toscana* samples (84.2%), with three EVOOs from *Toscana* classified as *Garda* and one *Garda* sample misclassified as *Sicilia*. Results confirm the effectiveness of the comprehensive volatiles fingerprinting for geographical classification of EVOOs [29,65].

By examining the variables importance in the projection (VIP) score, which summarizes the overall contribution of each variable to the PLS-DA model, components with a higher informative role in describing the characteristic regional signatures were selected. Those having VIP value ± SD higher than 1, were 27, of them 11 untargeted and 16 targeted. Within the identified analytes, those with the highest VIP ranking were: (*E)*-2-hexenal, phenylethyl alcohol, ethyl acetate, 1-penten-3-ol, butyl butanoate, 2-buten-1-ol, 2-ethylfuran, 1-pentanol, tridecane, (Z)-2-hexenal, (Z)-3-hexenol, butyrolactone, δ-3-carene, propanal, 3-pentanone, and α-farnesene.

Figure 3B shows the score plot resulting from the PLS-DA based on the 42 quantified compounds. Results of a full cross-validation (CV=4) performed on the entire sample set, gave an average sensitivity of 73.3% and specificity of 87.1%. Nearly all EVOOs from *Sicilia* were correctly classified (one misclassified as *Toscana*), whereas the number of misclassified samples between *Toscana* and *Garda* regions increased compared to the *UT* fingerprinting model. For targeted profiling data, the list of compounds selected by VIPs scores, in decreasing order of relevance for regional classification, were: (*E*)-2-hexenal, 1-penten-3-ol, 3-pentanone, 1-pentanol, (*Z*)-3-hexen-1-ol, α-copaene, ethyl acetate, and (*Z*)-3-hexenyl acetate. Score plot and performance parameters clearly show that the discrimination capacity of the model based on the quantified compounds was markedly lower. Analytes selection was in fact driven by their role in defining positive or negative attributes to the overall aroma and on analytical variables not necessarily related to the regional influence on volatiles expression (i.e., absence of HS saturation effect ($\beta < 0.95$) and co-elutions). However, results obtained by accurate MHS-SPME quantification are likely more robust, referable, and transferable in time and between different platforms.

Boxplots in Figure 4 show the quantitative distribution of selected EVOO volatiles from the three production

regions. Interestingly, discriminant compounds mostly belong to the LOX signature: (*E*)-2-hexenal is significantly higher in EVOOs from *Toscana* and *Garda* compared to *Sicilia*; (*Z*)-3-hexen-1-ol and 3-pentanone are more abundant in *Sicilia* samples, and hexyl acetate shows a higher amount in *Garda* and *Sicilia* compared to *Toscana* samples. The sesquiterpenoid α-copaene is more abundant in EVOOs from *Sicilia* and 1-pentanol is on average more concentrated in *Sicilia* samples.

3.5. Italian high-quality EVOO aroma blueprint

To develop a realistic picture about the sensory contribution of quantified analytes on the overall EVOO aroma, odor activity values (OAVs) might be useful. By molecular sensory science principles (*i.e.*, sensomics [23]), odorants having an OAV >1 and with positive validation in aroma recombinates are considered key-aromas [51]. Although this simplification could lead to a misleading interpretation of the actual role played by odor-active compounds in modulating the aroma perception of a food, the concept has been validated over hundreds of food products [23]. OAV is a robust yet objective tool to identify character odorants and to rank them over the multitude of volatiles characterizing a given product.

The relevance of quantitated analytes in terms of their sensory contribution to the aroma perception of EVOO samples is illustrated in spider-diagrams of **Figure 5.** Median values of OAVs for all potent odorants, *i.e.*, those reporting an OAV > 1 in at least one sample, are visualized for each production region (**Fig.5A** *Garda*, **Fig.5B** *Toscana*, and **Fig.5C** *Sicilia*) and in decreasing order of OAVs taking the *Garda* as reference. Analytes are accompanied by their odor descriptors. Pictograms clearly show differences in the aroma blueprints of EVOOs from these different regions.

In all regions, compounds belonging to the LOX signature and related to positive attributes as *pungent, green* and *grassy* notes, dominate the overall aroma of EVOOs, even if in different proportions; *e.g*., (E)-2-hexenal has higher OAV in *Garda* and *Toscana* than in *Sicilia*, whereas (Z)-3-hexenyl acetate has a higher impact on *Toscana* and *Sicilia* EVOOs aroma [40,69]). Compounds related to *fruity* notes, *e.g*. (Z)-3-hexen-1-ol, might evoke the perception of *banana-like* and *grassy* qualities, documented in EVOOs from *Sicilia* [69]. 1-Hexanol with *fruity* and *banana-like* perception has higher relevance in *Garda* and *Toscana* samples.

The important role of terpenoids, highlighted by profiling data as regional markers, is here seen in the OAVs for limonene and eucalyptol, likely contributing to the definition of *citrus, herbal, terpenic* qualities. Moreover, several EVOOs from the Garda lake area show α-pinene with an OAV > 1, likely eliciting *herbal* and *woody* notes.

Interestingly, among the 42 quantified analytes, only four are correlated to sensorial defects (*i.e.*, acetic acid, (*E,E*)-2,4-heptadienal, (*E*)-2-nonenal, and nonanal [24,35,36,39]) and only in a few samples is their OAV > 1. This result was expected in that the analyzed EVOOs had sensory classifications with the median of the coded defects equal to zero.

4. Conclusions

The possibility of performing highly informative chromatographic fingerprinting, extended to both untargeted and targeted volatile components, accompanied by accurate multi-target quantification performed on two parallel detection channels (MS/FID), has been demonstrated in the challenging context of high-quality EVOO valorization and characterization. Compared to existing methods based on 1D-GC-FID or 1D-GC-MS, the current procedure offers higher separation power and chromatographic resolution that improve method specificity and selectivity. Higher chromatographic effectiveness results in lower LODs and LOQs [27] and high quality calibration (*i.e*, R^2 and residual distribution [27]) provides accurate quantification in a wider range of concentrations. Moreover, parallel detection by MS/FID offers the possibility of cross-validation of quantitative results and the option of adopting FID RRFs to extend quantification to uncalibrated analytes.

The crucial yet fundamental role of an effective, fully automated, and highly repeatable sample preparation approach, *i.e.*, MHS-SPME, is further highlighted even in a "true" quantification approach by evidencing the inaccuracy of semi-quantitative methodologies (*e.g*, HS-SPME and IS normalization). By exploring the possibility of adopting MHS-SPME-GC×GC-MS/FID as artificial intelligence smelling machine [47] for EVOOs, it has been demonstrated how the great flexibility and reliability of multidimensional analytical techniques implemented with commercially available instrumentation can improve the quality and the information power of each analytical run.

Acknowledgments

The project was supported by Agilent Technologies (Wilmington, DE, USA) through its *Applications and Core Technology University Research* (ACT/UR) programme, Project ID: #4294, "Development and Validation of Novel Tools to Facilitate Conversion of Thermal Modulated GC×GC Methods to Reverse Flow Modulated GC×GC Methods."

Declaration of Competing Interest

The authors declare the following financial interests/personal relationships which may be considered as potential competing interests: Prof. Stephen E. Reichenbach has a financial interest in GC Image, LLC; Dr. James McCurry is employee of Agilent Technologies; and Dr. Daniela Peroni is employee of SRA Instruments a Premier Solution Partner of Agilent Technologies.

References

[1] F. Stilo, C. Bicchi, A. Robbat, S.E. Reichenbach, C. Cordero, Untargeted approaches in food-omics: the potential of comprehensive two-dimensional gas chromatography/mass spectrometry, TrAC Trends Anal. Chem. 135 (2020) 116162. doi:10.1016/j.trac.2020.116162.

[2] F. Stilo, C. Bicchi, A.M. Jimenez-Carvelo, L. Cuadros-Rodriguez, S.E. Reichenbach, C. Cordero, Chromatographic fingerprinting by comprehensive two-dimensional chromatography: Fundamentals and tools, TrAC - Trends Anal. Chem. 134 (2021) 116133. doi:10.1016/j.trac.2020.116133.

[3] C. Cordero, J. Kiefl, S.E. Reichenbach, C. Bicchi, Characterization of odorant patterns by comprehensive two-dimensional gas chromatography: A challenge in omic studies, TrAC - Trends Anal. Chem. 113 (2019) 364–378. doi:10.1016/j.trac.2018.06.005.

[4] P.Q. Tranchida, G. Purcaro, M. Maimone, L. Mondello, Impact of comprehensive two-dimensional gas chromatography with mass spectrometry on food analysis, J. Sep. Sci. 39 (2016) 149–161. doi:10.1002/jssc.201500379.

[5] F. Magagna, L. Valverde-Som, C. Ruíz-Samblás, L. Cuadros-Rodríguez, S.E. Reichenbach, C. Bicchi, C. Cordero, Combined untargeted and targeted fingerprinting with comprehensive two-dimensional chromatography for volatiles and ripening indicators in olive oil, Anal. Chim. Acta. 936 (2016) 245–258. doi:10.1016/j.aca.2016.07.005.

[6] S.E. Reichenbach, C.A. Zini, K.P. Nicolli, J.E. Welke, C. Cordero, Q. Tao, Benchmarking machine learning methods for comprehensive chemical fingerprinting and pattern recognition, J. Chromatogr. A. 1595 (2019) 158–167. doi:10.1016/j.chroma.2019.02.027.

[7] L. Nicolotti, C. Cordero, C. Cagliero, E. Liberto, B. Sgorbini, P. Rubiolo, C. Bicchi, Quantitative fingerprinting by headspace-Two-dimensional comprehensive gas chromatography-mass spectrometry of solid matrices: Some challenging aspects of the exhaustive assessment of food volatiles, Anal. Chim. Acta. 798 (2013) 115–125. doi:10.1016/j.aca.2013.08.052.

[8] C. Cordero, P. Rubiolo, S.E. Reichenbach, A. Carretta, L. Cobelli, M. Giardina, C. Bicchi, Method translation and full metadata transfer from thermal to differential flow modulated comprehensive two dimensional gas chromatography: Profiling of suspected fragrance allergens, J. Chromatogr. A. 1480 (2017) 70–82. doi:10.1016/j.chroma.2016.12.011.

[9] C. Cordero, P. Rubiolo, L. Cobelli, G. Stani, A. Miliazza, M. Giardina, R. Firor, C. Bicchi, Potential of the reversed-inject differential flow modulator for comprehensive two-dimensional gas chromatography in the quantitative profiling and fingerprinting of essential oils of different complexity, J. Chromatogr. A. 1417 (2015) 79–95. doi:10.1016/j.chroma.2015.09.027.

[10] F. Stilo, E. Gabetti, C. Bicchi, A. Carretta, D. Peroni, S.E. Reichenbach, C. Cordero, J. McCurry, A step forward in the equivalence between thermal and differential-flow modulated comprehensive two-dimensional gas chromatography methods, J. Chromatogr. A. 1627 (2020) 461396. doi:10.1016/j.chroma.2020.461396.

[11] F.A. Franchina, M. Maimone, P.Q. Tranchida, L. Mondello, Flow modulation comprehensive two-dimensional gas chromatography–mass spectrometry using ≈4 mL min−1 gas flows, J. Chromatogr. A. 1441 (2016) 134–139. doi:10.1016/j.chroma.2016.02.041.

[12] J. V. Seeley, N.J. Micyus, S. V. Bandurski, S.K. Seeley, J.D. McCurry, Microfluidic deans switch for comprehensive two-dimensional gas chromatography, Anal. Chem. 79 (2007) 1840–1847. doi:10.1021/ac061881g.

[13] J. V. Seeley, N.J. Micyus, J.D. McCurry, S.K. Seeley, Comprehensive two-dimensional gas chromatography with a simple fluidic modulator, Am. Lab. 38 (2006) 24–26.

[14] M.S. Klee, L.M. Blumberg, Theoretical and Practical Aspects of Fast Gas Chromatography and Method Translation, J. Chromatogr. Sci. 40 (2002) 234–247. doi:10.1093/chromsci/40.5.234.

[15] M. Giardina, J.D. McCurry, P. Cardinael, G. Semard-Jousset, C. Cordero, C. Bicchi, Development and validation of a pneumatic model for the reversed-flow differential flow modulator for comprehensive two-dimensional gas chromatography, J. Chromatogr. A. 1577 (2018) 72–81. doi:10.1016/j.chroma.2018.09.022.

[16] Eurachem, Eurachem Guide: The Fitness for Purpose of Analytical Methods – A Laboratory Guide to Method Validation and Related Topics., 2014. doi:978-91-87461-59-0.

[17] E. Commission, Commission Decision 2002/657/EC implementing Council Directive 96/23/EC concerning the performance of analytical methods and the interpretation of results, Off. J. Eur. Union. L221 (2002) 8–36. http://www.ecolex.org/ecolex/ledge/view/RecordDetails?id=LEX-FAOC049615&index=documents%5Cnfile://g/R&D/PAPE/articles/Mass Spec/European directive MS IP.pdf.

[18] D. Grigg, Olive oil, the Mediterranean and the world, GeoJournal. 53 (2001) 163–172. doi:10.1023/A:1015702327546.

[19] L. Cecchi, M. Migliorini, E. Giambanelli, A. Rossetti, A. Cane, F. Melani, N. Mulinacci, Headspace Solid-Phase Microextraction-Gas Chromatography-Mass Spectrometry Quantification of the Volatile Profile of More than 1200 Virgin Olive Oils for Supporting the Panel Test in Their Classification: Comparison of Different Chemometric Approaches, J. Agric. Food Chem. 67 (2019) 9112–9120. doi:10.1021/acs.jafc.9b03346.

[20] IOC, International Olive Council, Newsl. No 144 DECEMBER 2019. (2019).

[21] European Union, EU quality schemes, (2020). https://ec.europa.eu/info/food-farming-fisheries/food-safety-and-quality/certification/quality-labels/quality-schemes-explained_en.

[22] L. Cuadros-Rodríguez, C. Ruiz-Samblás, L. Valverde-Som, E. Pérez-Castaño, A. González-Casado,

Chromatographic fingerprinting: An innovative approach for food “identitation” and food authentication - A tutorial, Anal. Chim. Acta. 909 (2016) 9–23. doi:10.1016/j.aca.2015.12.042.

[23] A. Dunkel, M. Steinhaus, M. Kotthoff, B. Nowak, D. Krautwurst, P. Schieberle, T. Hofmann, Nature’s chemical signatures in human olfaction: A foodborne perspective for future biotechnology, Angew. Chemie - Int. Ed. 53 (2014) 7124–7143. doi:10.1002/anie.201309508.

[24] G. Purcaro, C. Cordero, E. Liberto, C. Bicchi, L.S. Conte, Toward a definition of blueprint of virgin olive oil by comprehensive two-dimensional gas chromatography, J. Chromatogr. A. 1334 (2014) 101–111. doi:10.1016/j.chroma.2014.01.067.

[25] E. Belhassen, D. Bressanello, P. Merle, E. Raynaud, C. Bicchi, A. Chaintreau, C. Cordero, Routine quantification of 54 allergens in fragrances using comprehensive two-dimensional gas chromatography-quadrupole mass spectrometry with dual parallel secondary columns. Part I: Method development, Flavour Fragr. J. 33 (2018) 63–74. doi:10.1002/ffj.3416.

[26] C. Cordero, A. Guglielmetti, B. Sgorbini, C. Bicchi, E. Allegrucci, G. Gobino, L. Baroux, P. Merle, Odorants quantitation in high-quality cocoa by multiple headspace solid phase micro-extraction: Adoption of FID-predicted response factors to extend method capabilities and information potential, Anal. Chim. Acta. 1052 (2019). doi:10.1016/j.aca.2018.11.043.

[27] E. Casadei, E. Valli, R. Aparicio-Ruiz, C. Ortiz-Romero, D.L. García-González, S. Vichi, B. Quintanilla-Casas, A. Tres, A. Bendini, T.G. Toschi, Peer inter-laboratory validation study of a harmonized SPME-GC-FID method for the analysis of selected volatile compounds in virgin olive oils, Food Control. 123 (2021). doi:10.1016/j.foodcont.2020.107823.

[28] S. Vichi, L. Pizzale, L.S. Conte, S. Buxaderas, E. López-Tamames, Solid-Phase Microextraction in the Analysis of Virgin Olive Oil Volatile Fraction: Characterization of Virgin Olive Oils from Two Distinct Geographical Areas of Northern Italy, J. Agric. Food Chem. 51 (2003) 6572–6577. doi:10.1021/jf030269c.

[29] B. Quintanilla-Casas, J. Bustamante, F. Guardiola, D.L. García-González, S. Barbieri, A. Bendini, T.G. Toschi, S. Vichi, A. Tres, Virgin olive oil volatile fingerprint and chemometrics: Towards an instrumental screening tool to grade the sensory quality, LWT. 121 (2020) 108936. doi:https://doi.org/10.1016/j.lwt.2019.108936.

[30] B. Quintanilla-Casas, M. Marin, F. Guardiola, D.L. García-González, S. Barbieri, A. Bendini, T.G. Toschi, S. Vichi, A. Tres, Supporting the sensory panel to grade virgin olive oils: an in-house-validated screening tool by volatile fingerprinting and chemometrics, Foods. 9 (2020) 1–14. doi:10.3390/foods9101509.

[31] L.T. Vaz-Freire, M.D.R.G. da Silva, A.M.C. Freitas, Comprehensive two-dimensional gas chromatography for fingerprint pattern recognition in olive oils produced by two different techniques in Portuguese olive varieties Galega Vulgar, Cobrançosa e Carrasquenha, Anal. Chim. Acta. 633 (2009) 263–270.

doi:10.1016/j.aca.2008.11.057.

[32] F. Stilo, E. Liberto, S.E. Reichenbach, Q. Tao, C. Bicchi, C. Cordero, Untargeted and Targeted Fingerprinting of Extra Virgin Olive Oil Volatiles by Comprehensive Two-Dimensional Gas Chromatography with Mass Spectrometry: Challenges in Long-Term Studies, J. Agric. Food Chem. 67 (2019) 5289–5302. doi:10.1021/acs.jafc.9b01661.

[33] EU Food Quality Labels, EU Food Qual. Labels. (2021). https://ec.europa.eu/info/news/new-search-database-geographical-indications-eu-2020-nov-25_en (accessed February 3, 2021).

[34] Progetto Ager, Violin project, (2016). https://olivoeolio.progettoager.it/index.php/olio-e-olivo-per-la-ricerca/itemlist/user/49-violin.

[35] A. Neugebauer, M. Granvogl, P. Schieberle, Characterization of the Key Odorants in High-Quality Extra Virgin Olive Oils and Certified Off-Flavor Oils to Elucidate Aroma Compounds Causing a Rancid Off-Flavor, J. Agric. Food Chem. 68 (2020) 5927–5937. doi:10.1021/acs.jafc.0c01674.

[36] C.M. Kalua, M.S. Allen, D.R. Bedgood, A.G. Bishop, P.D. Prenzler, K. Robards, Olive oil volatile compounds, flavour development and quality: A critical review, Food Chem. 100 (2007) 273–286. doi:10.1016/j.foodchem.2005.09.059.

[37] F. Stilo, C. Cordero, B. Sgorbini, C. Bicchi, E. Liberto, Highly Informative Fingerprinting of Extra-Virgin Olive Oil Volatiles: The Role of High Concentration-Capacity Sampling in Combination with Comprehensive Two-Dimensional Gas Chromatography, Separations. 6 (2019) 34. doi:10.3390/separations6030034.

[38] F. Angerosa, Influence of volatile compounds on virgin olive oil quality evaluated by analytical approaches and sensor panels, Eur. J. Lipid Sci. Technol. 104 (2002) 639–660. doi:10.1002/1438-9312(200210)104:9/10<639::AID-EJLT639>3.0.CO;2-U.

[39] M.T. Morales, G. Luna, R. Aparicio, Comparative study of virgin olive oil sensory defects, Food Chem. 91 (2005) 293–301. doi:10.1016/j.foodchem.2004.06.011.

[40] E. Aprea, F. Gasperi, E. Betta, G. Sani, C. Cantini, Variability in volatile compounds from lipoxygenase pathway in extra virgin olive oils from tuscan olive germoplasm by quantitative SPME/GC-MS, J. Mass Spectrom. 53 (2018) 824–832. doi:10.1002/jms.4274.

[41] L. Cecchi, M. Migliorini, N. Mulinacci, Virgin Olive Oil Volatile Compounds: Composition, Sensory Characteristics, Analytical Approaches, Quality Control, and Authentication, J. Agric. Food Chem. (2021). doi:10.1021/acs.jafc.0c07744.

[42] Y. Wang, J. O'Reilly, Y. Chen, J. Pawliszyn, Equilibrium in-fibre standardisation technique for solid-phase microextraction, J. Chromatogr. A. 1072 (2005) 13–17. doi:10.1016/j.chroma.2004.12.084.

[43] S. Vichi, J.M. Guadayol, J. Caixach, E. Lopeztamames, S. Buxaderas, E. López-Tamames, S. Buxaderas,

Comparative study of different extraction techniques for the analysis of virgin olive oil aroma, Food Chem. 105 (2007) 1171–1178. doi:10.1016/j.foodchem.2007.02.018.

[44] C. Cordero, C. Cagliero, E. Liberto, L. Nicolotti, P. Rubiolo, B. Sgorbini, C. Bicchi, High concentration capacity sample preparation techniques to improve the informative potential of two-dimensional comprehensive gas chromatography-mass spectrometry: Application to sensomics, J. Chromatogr. A. 1318 (2013) 1–11. doi:10.1016/j.chroma.2013.09.065.

[45] F. Stilo, E. Liberto, S.E. Reichenbach, Q. Tao, C. Bicchi, C. Cordero, Exploring the extra-virgin olive oil volatilome by adding extra dimensions to comprehensive two-dimensional gas chromatography and time of flight mass spectrometry featuring tandem ionization: validation of ripening markers in headspace linearity conditio, J. AOAC Int. (2020) 1–14. doi:10.1093/jaoacint/qsaa095.

[46] B. Kolb, L.S. Ettre, Static headspace-gas chromatography : theory and practice, Wiley-VCH, New York, 2006. https://books.google.com/books?hl=en&lr=&id=nGPmpb4VvEgC&oi=fnd&pg=PR5&ots=6SZHNIygx6&sig=lcvdWEsXW-3H8BzCWuKuK2Pnjil#v=onepage&q&f=false.

[47] L. Nicolotti, V. Mall, P. Schieberle, Characterization of Key Aroma Compounds in a Commercial Rum and an Australian Red Wine by Means of a New Sensomics-Based Expert System (SEBES) - An Approach to Use Artificial Intelligence in Determining Food Odor Codes, J. Agric. Food Chem. 67 (2019) 4011–4022. doi:10.1021/acs.jafc.9b00708.

[48] C. Bicchi, M.R. Ruosi, C. Cagliero, C. Cordero, E. Liberto, P. Rubiolo, B. Sgorbini, Quantitative analysis of volatiles from solid matrices of vegetable origin by high concentration capacity headspace techniques: Determination of furan in roasted coffee, J. Chromatogr. A. 1218 (2011) 753–762. doi:10.1016/j.chroma.2010.12.002.

[49] J. Pawliszyn, C.F. Ross, Headspace Analysis, in: Compr. Sampl. Sample Prep., Elsevier, 2012: pp. 27–50. doi:10.1016/B978-0-12-381373-2.10036-5.

[50] B. Sgorbini, C. Cagliero, E. Liberto, P. Rubiolo, C. Bicchi, C.E.I. Cordero, Strategies for Accurate Quantitation of Volatiles from Foods and Plant-Origin Materials: A Challenging Task, J. Agric. Food Chem. (2019) 1619–1630. doi:10.1021/acs.jafc.8b06601.

[51] C. Cordero, A. Guglielmetti, B. Sgorbini, C. Bicchi, E. Allegrucci, G. Gobino, L. Baroux, P. Merle, Odorants quantitation in high-quality cocoa by multiple headspace solid phase micro-extraction: Adoption of FID-predicted response factors to extend method capabilities and information potential, Anal. Chim. Acta. 1052 (2019) 190–201. doi:10.1016/J.ACA.2018.11.043.

[52] B. Kolb, L.S. Ettre, Theory and practice of multiple headspace extraction, Chromatographia. 32 (1991) 505–513. doi:10.1007/BF02327895.

[53] M. Suzuki, S. Tsuge, T. Takeuchi, Gas Chromatographic Estimation of Occluded Solvents in Adhesive Tape by Periodic Introduction Method, Anal. Chem. 42 (1970) 1705–1708. doi:10.1021/ac50160a035.

[54] MCAULLIFE C, GC determination of solutes by multiple phase equilibration, Chem. Tech. (1971) 46–51.

[55] B. Sgorbini, C. Bicchi, C. Cagliero, C. Cordero, E. Liberto, P. Rubiolo, Herbs and spices: Characterization and quantitation of biologically-active markers for routine quality control by multiple headspace solid-phase microextraction combined with separative or non-separative analysis, J. Chromatogr. A. 1376 (2015) 9–17. doi:10.1016/j.chroma.2014.12.007.

[56] R. Costa, L. Tedone, S. De Grazia, P. Dugo, L. Mondello, Multiple headspace-solid-phase microextraction: An application to quantification of mushroom volatiles, Anal. Chim. Acta. 770 (2013) 1–6. doi:10.1016/j.aca.2013.01.041.

[57] Ó. Ezquerro, G. Ortiz, B. Pons, M.T. Tena, Determination of benzene, toluene, ethylbenzene and xylenes in soils by multiple headspace solid-phase microextraction, J. Chromatogr. A. 1035 (2004) 17–22. doi:10.1016/j.chroma.2004.02.030.

[58] W.-Q. Xie, Y.-X. Gong, K.-X. Yu, Enhancing the Sensitivity of Full Evaporation Technique Using Multiple Headspace Extraction Analysis, Chromatographia. 80 (2017) 1263–1268. doi:10.1007/s10337-017-3343-x.

[59] T. Wenzl, J. Haedrich, A. Schaechtele, P. Robouch, J. Stroka, Guidance Document on the Estimation of LOD and LOQ for Measurements in the Field of Contaminants in Feed and Food. EUR 28099 EN, 2016. doi:10.2787/8931.

[60] C. Cordero, J. Kiefl, P. Schieberle, S.E. Reichenbach, C. Bicchi, Comprehensive two-dimensional gas chromatography and food sensory properties: Potential and challenges, Anal. Bioanal. Chem. 407 (2015) 169–191. doi:10.1007/s00216-014-8248-z.

[61] J.Y. De Saint Laumer, S. Leocata, E. Tissot, L. Baroux, D.M. Kampf, P. Merle, A. Boschung, M. Seyfried, A. Chaintreau, Prediction of response factors for gas chromatography with flame ionization detection: Algorithm improvement, extension to silylated compounds, and application to the quantification of metabolites, J. Sep. Sci. 38 (2015) 3209–3217. doi:10.1002/jssc.201500106.

[62] L. Cecchi, M. Migliorini, E. Giambanelli, A. Rossetti, A. Cane, N. Mulinacci, New Volatile Molecular Markers of Rancidity in Virgin Olive Oils under Nonaccelerated Oxidative Storage Conditions, J. Agric. Food Chem. 67 (2019) 13150–13163. doi:10.1021/acs.jafc.9b05809.

[63] F. Angerosa, M. Servili, R. Selvaggini, A. Taticchi, S. Esposto, G. Montedoro, Volatile compounds in virgin olive oil: Occurrence and their relationship with the quality, J. Chromatogr. A. 1054 (2004) 17–31. doi:10.1016/j.chroma.2004.07.093.

[64] A. Genovese, N. Caporaso, T. Leone, A. Paduano, C. Mena, M.A. Perez-Jimenez, R. Sacchi, Use of odorant

series for extra virgin olive oil aroma characterisation, J. Sci. Food Agric. 99 (2019) 1215–1224. doi:10.1002/jsfa.9293.

[65] B. Quintanilla-Casas, S. Bertin, K. Leik, J. Bustamante, F. Guardiola, E. Valli, A. Bendini, T.G. Toschi, A. Tres, S. Vichi, Profiling versus fingerprinting analysis of sesquiterpene hydrocarbons for the geographical authentication of extra virgin olive oils, Food Chem. 307 (2020). doi:10.1016/j.foodchem.2019.125556.

[66] J.F. Cavalli, X. Fernandez, L. Lizzani-Cuvelier, A.M. Loiseau, Characterization of volatile compounds of French and Spanish virgin olive oils by HS-SPME: Identification of quality-freshness markers, Food Chem. 88 (2004) 151–157. doi:10.1016/j.foodchem.2004.04.003.

[67] R. Aparicio, M.T. Morales, R. Aparicio-Ruiz, N. Tena, D.L. García-González, Authenticity of olive oil: Mapping and comparing official methods and promising alternatives, Food Res. Int. 54 (2013) 2025–2038. doi:10.1016/j.foodres.2013.07.039.

[68] R. Hachicha Hbaieb, F. Kotti, M. Gargouri, M. Msallem, S. Vichi, Ripening and storage conditions of Chétoui and Arbequina olives: Part I. Effect on olive oils volatiles profile, Food Chem. 203 (2016) 548–558. doi:10.1016/j.foodchem.2016.01.089.

[69] A. Da Ros, D. Masuero, S. Riccadonna, K.B. Bubola, N. Mulinacci, F. Mattivi, I. Lukić, U. Vrhovsek, Complementary untargeted and targeted metabolomics for differentiation of extra virgin olive oils of different origin of purchase based on volatile and phenolic composition and sensory quality, Molecules. 24 (2019) 1–17. doi:10.3390/molecules24162896.

Table captions

Table 1. List of analyzed samples together with harvest region/origin, identification codes, olives cultivar, and EU quality labelling and/or additional certifications (*i.e.*, organic cultivation and production).

Table 2. List of the fifteen target odorants together with their odor quality, odor threshold in oil as reported in literature (OT ng/g), experimental I^T, target ion used for quantification (Ti), additional qualifier ions (Q#n), calibration range covered, calibration function for MS and FID channels with the corresponding determination coefficient (R^2), intermediate precision data expressed as % relative standard deviation (RSD %) obtained by replicated quantitative measurements on a representative sample, limit of detection (LOD) and limit of quantification (LOQ).

Table 3. Extended list of target analytes, reported with their experimental I^T, molecular weight (MW) and molecular formula. Relative Response Factors (RRF) are calculated based on Equation 3. β values (± SD) are calculated on the entire sample set while accuracy data is reported as Relative Error (RE%) on calibration solutions at 25 ng (CS25) by MHS-SPME and between MHS-SPME and HS-SPME with IS normalization on FID signals.

Figure captions

Figure 1: pseudocolor images of the volatiles pattern of S#1 EVOO sample from *Sicilia* analyzed by a polar × semi-polar column combination (*i.e.*, PEG × OV1701) and resulting from the parallel detection by MS (**1A**) and FID (**1B**). Enlarged areas of the chromatographic plane (red rectangles in quadrant *I* - **1C**, *II* - **1D**, and *III* - **1E**) highlights the complexity of the pattern and the chromatographic resolution of analytes clusters.

Figure 2: Histograms illustrating accuracy of MHS-SPME *vs.* HS-SPME with IS normalization on (**2A**) the 25 ng CS (blue and orange bars). Expected values (*i.e.*, 25 ng) are marked with a green line while boundary highlights a ± 20% error tolerance. In **2B**, accuracy is shown for a EVOO sample. Results correspond to the average values of replicated analyses (n=3).

Figure 3: PLS-DA score plots resulting from the model for regional discrimination of samples and based on the UT peaks responses (**3A**) or quantitated target compounds from Table 3 (**3B**).

Figure 4: Box-plots illustrating the median, minimum and maximum and mean quantitative values (red mark) for discriminant targeted compounds.

Figure 5: Spider-diagrams showing the EVVOs aroma blueprint and based on calculated OAVs (reported in logarithmic scale). Key-aroma compounds are reported in descending order taking the Garda lake group as reference. Odor qualities are also indicated.

Table 1. List of analyzed samples with harvest region/origin, identification codes, olives cultivar, and EU quality labelling and/or additional certifications (i.e., organic cultivation and production).

Origin	Sample ID	Cultivar	Additional qualifications
Garda	G1	*Leccino*	PDO
	G2	*Casaliva, Leccino*	PDO
	G3	*Casaliva, Leccino*	PDO
	G4	*Casaliva, Leccino*	PDO
	G5	*Casaliva, Leccino, Moraiolo, Pendolino*	PDO
	G6	*Casaliva*	PDO
	G7	*Casaliva, Frantoio, Leccino*	
	G8	*Coratina*	
	G9	*Grignano*	
	G10	*Grignano, Favarol, Pendolino, Trepp*	PDO
	G11	Blend	
	G12	*Casaliva*	Organic
	G13	*Casaliva, Frantoio, Leccino*	PDO
	G14	*Casaliva, Frantoio, Leccino*	
	G15	*Casaliva*	
Sicilia	S1	*Nocellara del Belice*	
	S2	*Nocellara del Belice*	Organic
	S3	*Cerasuola e Nocellara del Belice*	Organic
	S4	Blend	PDO
	S5	*Nocellara del Belice*	
	S6	*Tonda Iblea*	
	S7	*Cerasuola, Nocellara del Belice, Biancolilla*	PGI
	S8	*Nocellara del Belice*	PDO
	S9	*Biancolilla*	PDO
	S10	*Nocellara del Belice*	PDO
	S11	*Tonda Iblea*	PDO
	S12	*Nocellara Messinese*	
	S13	*Nocellara Etnea*	
	S14	*Nocellara Etnea*	
	S15	*Nocellara del Belice*	
	S16	*Nocellara del Belice*	
	S17	*Biancolilla*	
	S18	*Cerasuola*	
Toscana	T1	*Frantoio, Moraiolo, Maurino, Picholine*	
	T2	Blend	PGI
	T3	Blend	Organic
	T4	Blend	PDO
	T5	Blend	PGI
	T6	Blend	PGI
	T7	Blend	Organic, PGI
	T8	*Moraiolo, Frantoio, Leccino, Americano*	Organic
	T9	*Frantoio, Moraiolo, Leccino*	PGI
	T10	*Moraiolo*	PGI
	T11	Blend	
	T12	*Olivastra Saggianese*	PDO
	T13	*Olivastra Saggianese*	PDO
	T14	Blend	PDO
	T15	*Correggiolo, Leccino, Frantoio*	PDO
	T16	*Frantoio, Leccino, Moraiolo*	
	T17	*Frantoio, Leccino, Moraiolo, Pendolino*	

Table 2. List of the fifteen targeted odorants with their odor quality, odor threshold in oil as reported in literature (OT ng/g), experimental I^T, target ion used for quantification (Ti), additional qualifier ions (Q#n), calibration range covered, calibration function for MS and FID channels with the corresponding determination coefficient (R^2), intermediate precision data expressed as % relative standard deviation (RSD %) obtained by replicated quantitative measurements on a representative sample, limit of detection (LOD), and limit of quantification (LOQ).

							MHS-SPME calibration MS				MHS-SPME calibration FID					
Targeted analyte	Odor quality	OT (ng/g)	Exp. I^T	Ti (m/z)	Q#n (m/z)	Range (ng)	Regression equation			Precision	Regression equation			Precision	LOD (ng/g)	LOQ (ng/g)
							m	*q*	R^2	RSD%	*m*	*q*	R^2	RSD%		
Ethyl acetate	Fruity, sweet, winey	940[§]	865	70	88;61	1-5	0.26	0.81	0.996	9.2	0.10	0.03	1	8.9	0.47	1.57
						5-100	0.40	0.11	0.995		0.81	2.38	0.996			
Hexanal	Green-apple, grass	300[$]	1072	72	82;56	1-10	0.85	1.00	0.995	9.5	1.34	1.44	0.998	9.8	0.33	1.1
						10-150	0.64	4.52	0.993		0.74	7.23	0.995			
2-Pentanol	Musty, fermented	380[£]	1095	73	87;55;45	1-100	1.61	0.79	0.997	7	0.98	0.68	0.996	9.7	0.16	0.53
(E)-2-Pentenal	Pungent, apple-like	300[§]	1121	84	69;55	1-5	1.07	0.11	0.995	3.7	0.34	0.16	0.996	2.9	0.47	1.57
						5-125	1.17	0.74	0.995		1.10	0.22	0.995			
1-Penten-3-ol	Pungent, butter	400[§]	1151	57	86;71	1-100	2.08	0.41	0.996	9.6	1.19	0.49	0.998	7.3	0.34	1.13
Heptanal	Citrus-like, fatty	500[$]	1179	96	81;70;55	1-125	0.99	0.95	0.999	1.9	1.18	0.86	0.997	4.9	0.22	0.73
(E)-2-Hexenal	Bitter almond, green, fruity	320[$]	1213	83	98;69;55	1-5	0.82	0.00	0.995	6.2	0.12	0.01	1	4.3	0.32	1.07
						5-125	0.93	0.16	0.995		1.38	0.20	0.995			
1-Pentanol	Sweet, pungent	470[§]	1240	70	87;55	1-5	1.35	0.03	0.995	2.4	0.21	0.02	0.999	4.2	0.39	1.3
						5-125	1.16	0.20	0.997		1.25	0.29	0.996			
(Z)-2-Penten-1-ol	Green, almond	250[£]	1306	68	86;57	1-125	1.60	0.09	0.997	2.6	1.27	0.32	0.996	6.3	0.29	0.97
(E)-2-Penten-1-ol	Mushroom, earthy	250[£]	1314	68	86;57	1-125	1.36	0.95	0.998	1.7	1.02	0.46	0.995	2.1	0.47	1.57
1-Hexanol	Fruity, banana, soft	400[§]	1346	84	102;69;56	1-5	1.49	0.15	0.996	7.8	0.24	0.01	1	3.8	0.26	0.87
						5-125	2.05	2.09	0.999		1.51	0.15	0.997			
(Z)-(3)-Hexen-1-ol	Banana, fresh, grass	1100[£]	1379	67	100;82;55	1-125	1.62	0.36	0.995	2.7	1.51	1.30	0.995	3.6	0.32	1.07
(E,E)-2,4-Hexadienal	Green	270[£]	1400	81	96;67;53	1-125	1.68	3.83	0.995	7.4	2.26	1.40	0.996	5.1	0.29	0.97
(E)-2-Octenal	Fatty, nutty	120[$]	1428	83	97;70;55	1-125	1.00	2.03	0.995	9.1	1.26	1.94	0.996	7.8	0.32	1.07
(E)-2-Nonenal	Fatty, green, soapy	140[$]	1534	96	111;83;70	1-100	0.27	0.56	0.991	3.5	1.14	2.01	0.998	4	0.07	0.23

§ G. Luna, M.T. Morales, R. Aparicio, Characterisation of 39 varietal virgin olive oils by their volatile compositions, Food Chem. 98 (2006) 243–252. https://doi.org/10.1016/j.foodchem.2005.05.069

$ A. Neugebauer, M. Granvogl, P. Schieberle, Characterization of the Key Odorants in High Quality Extra Virgin Olive Oils and Certified Off-Flavor Oils to Elucidate Aroma Compounds Causing a Rancid Off-Flavor, J. Agric. Food Chem. (2020) acs.jafc.0c01674. https://doi.org/10.1021/acs.jafc.0c01674.

£ L.J. Van Gemert, Odour Thresholds - Compilations of odour thresholds values in air, water and other media, 2011.

Table 3. Extended list of targeted analytes, reported with their experimental I^T, molecular weight (MW) and molecular formula. Relative Response Factors (RRF) are calculated based on Equation 1 and are normalized over 1-hexanol taken as internal reference. β values (± SD) are calculated on the entire sample set while accuracy data is reported as Relative Error (RE%) on calibration solutions at 25 ng (CS25) by MHS-SPME and between MHS-SPME and HS-SPME with IS normalization on FID signals.

			Predicted Relative Response Factor data							MHS-SPME vs. HS-SPME accuracy		
Targeted analytes	Exp. I^T	MW	Formula	η_C	η_H	η_O	η_{Benz}	RRF	β (±SD)	Relative Error % - CS25 MHS-SPME FID *vs*. MS	Amount µg/kg MHS-SPME	Amount µg/kg HS-SPME IS
Propanal	802	58.1	C_3H_6O	3	6	1	0	1.92	0.54 (±0.07)	-	86	134
Ethyl acetate	865	88.1	$C_4H_8O_2$	4	8	2	0	2.23	0.87 (±0.08)	9	133	103
3-Pentanone	956	86.1	$C_5H_{10}O$	5	10	1	0	1.49	0.52 (±0.05)	-	1775	741
1-Penten-3-one	1007	84.1	C_5H_8O	5	8	1	0	1.56	0.51 (±0.05)	-	50	182
α-Pinene	1026	136.2	$C_{10}H_{16}$	10	16	0	0	1.11	0.82 (±0.07)	-	910	88
Hexanal	1072	100.2	$C_6H_{12}O$	6	12	1	0	1.40	0.61 (±0.03)	8	461	2083
Camphene	1078	136.2	$C_{10}H_{16}$	10	16	0	0	1.11	0.83 (±0.05)	-	12	3
2-Pentanol	1107	88.2	$C_5H_{12}O$	5	12	1	0	1.42	0.77 (±0.11)	6	17	17
(E)-2-Pentenal	1121	84.1	C5H8O	5	8	1	0	1.56	0.53 (±0.02)	6	122	228
β-Pinene	1129	136.2	$C_{10}H_{16}$	10	16	0	0	1.11	0.92 (±0.06)	-	29	12
(Z)-3-Hexenal	1132	98.1	$C_6H_{10}O$	6	10	1	0	1.45	0.74 (±0.03)	-	44	26
δ-3-Carene	1150	136.2	$C_{10}H_{16}$	10	16	0	0	1.11	0.90 (±0.04)	-	2	7
1-Penten-3-ol	1151	86.1	$C_5H_{10}O$	5	10	1	0	1.49	0.62 (±0.02)	11	259	1327
Heptanal	1179	114.2	$C_7H_{14}O$	7	14	1	0	1.34	0.82 (±0.05)	3	18	16
Limonene	1190	136.2	$C_{10}H_{16}$	10	16	0	0	1.11	0.92 (±0.06)	-	125	53
Eucalyptol	1205	154.3	$C_{10}H_{18}O$	10	18	1	0	1.26	0.94 (±0.03)	-	596	3807
(E)-2-Hexenal	1213	98.1	$C_6H_{10}O$	6	10	1	0	1.45	0.63 (±0.02)	8	1981	3814
1-Pentanol	1240	88.2	$C_5H_{12}O$	5	12	1	0	1.42	0.71 (±0.03)	3	52	38
Hexyl acetate	1271	144.2	$C_8H_{16}O_2$	8	16	2	0	1.52	0.88 (±0.08)	-	20	155
Octanal	1285	128.2	$C_8H_{16}O$	8	16	1	0	1.29	0.94 (±0.04)	-	10	17
(Z)-2-Penten-1-ol	1306	86.1	$C_5H_{10}O$	5	10	1	0	1.49	0.61 (±0.02)	1	82	450
(E)-2-Penten-1-ol	1314	86.1	$C_5H_{10}O$	5	10	1	0	1.49	0.65 (±0.03)	1	18	43
(Z)-3-Hexenyl acetate	1317	142.2	$C_8H_{14}O_2$	8	14	2	0	1.57	0.89 (±0.04)	-	119	1245
(E)-2-Heptenal	1321	112.2	$C_7H_{12}O$	7	12	1	0	1.38	0.87 (±0.05)	-	14	39
6-Methyl-5-hepten-2-one	1327	126.2	$C_8H_{14}O$	8	14	1	0	1.33	0.91 (±0.03)	-	24	25
1-Hexanol	1346	102.2	$C_6H_{14}O$	6	14	1	0	1.35	0.79 (±0.02)	3	192	713

(Z)-(3)-Hexen-1-ol	1379	100.2	$C_6H_{12}O$	6	12	1	0	1.40	0.75 (±0.01)	7	466	1943
Nonanal	1393	142.2	$C_9H_{18}O$	9	18	1	0	1.26	0.95 (±0.02)	-	27	58
(E,E)-2,4-Hexadienal	1400	96.1	C_6H_8O	6	8	1	0	1.51	0.81 (±0.12)	10	69	290
(E)-2-Hexen-1-ol	1401	100.2	$C_6H_{12}O$	6	12	1	0	1.40	0.83 (±0.07)	-	824	776
Acetic acid	1409	60.1	$C_2H_4O_2$	2	4	2	0	5.06	0.78 (±0.09)	-	426	140
(E)-2-Octenal	1428	126.2	$C_8H_{14}O$	8	14	1	0	1.33	0.95 (±0.04)	10	47	5
(E,E)-2,4-Heptadienal	1464	110.2	$C_7H_{10}O$	7	10	1	0	1.42	0.86 (±0.05)	-	24	29
α-Copaene	1491	204.4	$C_{15}H_{24}$	15	24	0	0	1.09	0.77 (±0.06)	-	53	119
Benzaldehyde	1524	106.1	C_7H_6O	7	6	1	1	1.28	0.91 (±0.04)	-	13	31
(E)-2-Nonenal	1534	140.2	$C_9H_{16}O$	9	16	1	0	1.29	0.95 (±0.02)	15	22	4
Propanoic acid	1539	74.1	$C_3H_6O_2$	3	6	2	0	2.88	0.86 (±0.05)	-	54	17
1-Octanol	1551	130.2	$C_8H_{18}O$	8	18	1	0	1.26	0.95 (±0.03)	-	7	17
Butanoic acid	1578	88.1	$C_4H_8O_2$	4	8	2	0	2.23	0.93 (±0.05)	-	9	3
Butyrolactone	1613	86.1	$C_4H_6O_2$	4	6	2	0	2.43	0.92 (±0.04)	-	37	27
γ-Hexalactone	1670	114.1	$C_{10}H_{18}O_2$	10	18	2	0	0.96	0.94 (±0.03)	-	12	2
α-Farnesene	1753	204.4	$C_{15}H_{24}$	15	24	0	0	1.09	0.78 (±0.03)	-	7	17

Figure 1: Pseudocolor images of the volatiles pattern of S#1 EVOO sample from *Sicilia* analyzed by a polar × semi-polar column combination (i.e., PEG × OV1701) and resulting from the parallel detection by MS (**A**) and FID (**B**). Enlarged areas of the chromatographic plane (red rectangles *I* - **1C**, *II* - **1D**, and *III* - **1E**) highlight the complexity of the patterns and the chromatographic resolution of analyte clusters.

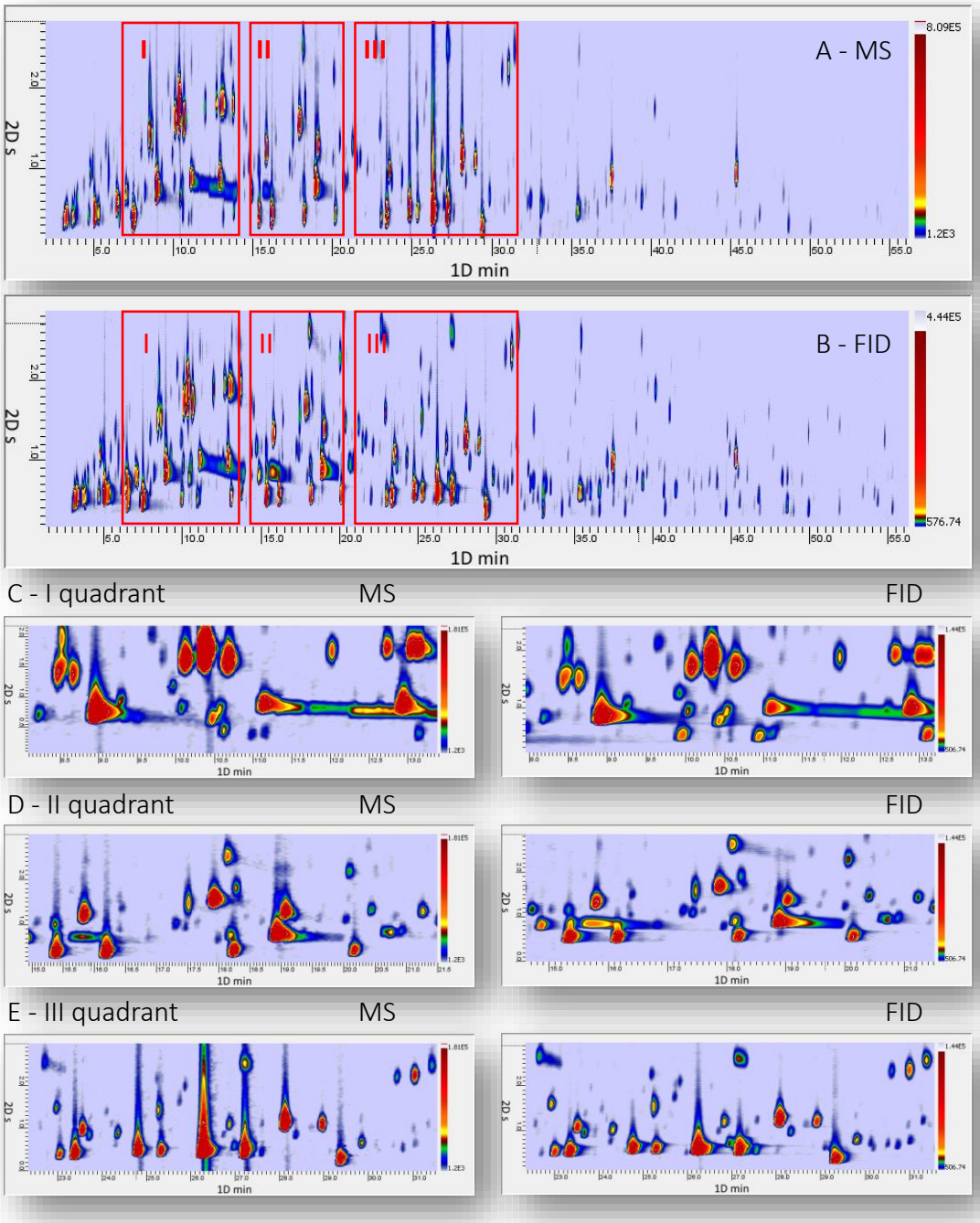

Figure 2: Histograms illustrating accuracy of MHS-SPME *vs.* HS-SPME with IS normalization on (**2A**) the 25 ng CS (blue and orange bars). Expected values (i.e., 25 ng) are marked with a green line while boundary highlights a ± 20% error tolerance. In **2B**, accuracy is shown for a EVOO sample. Results correspond to the average values of replicated analyses (n=3).

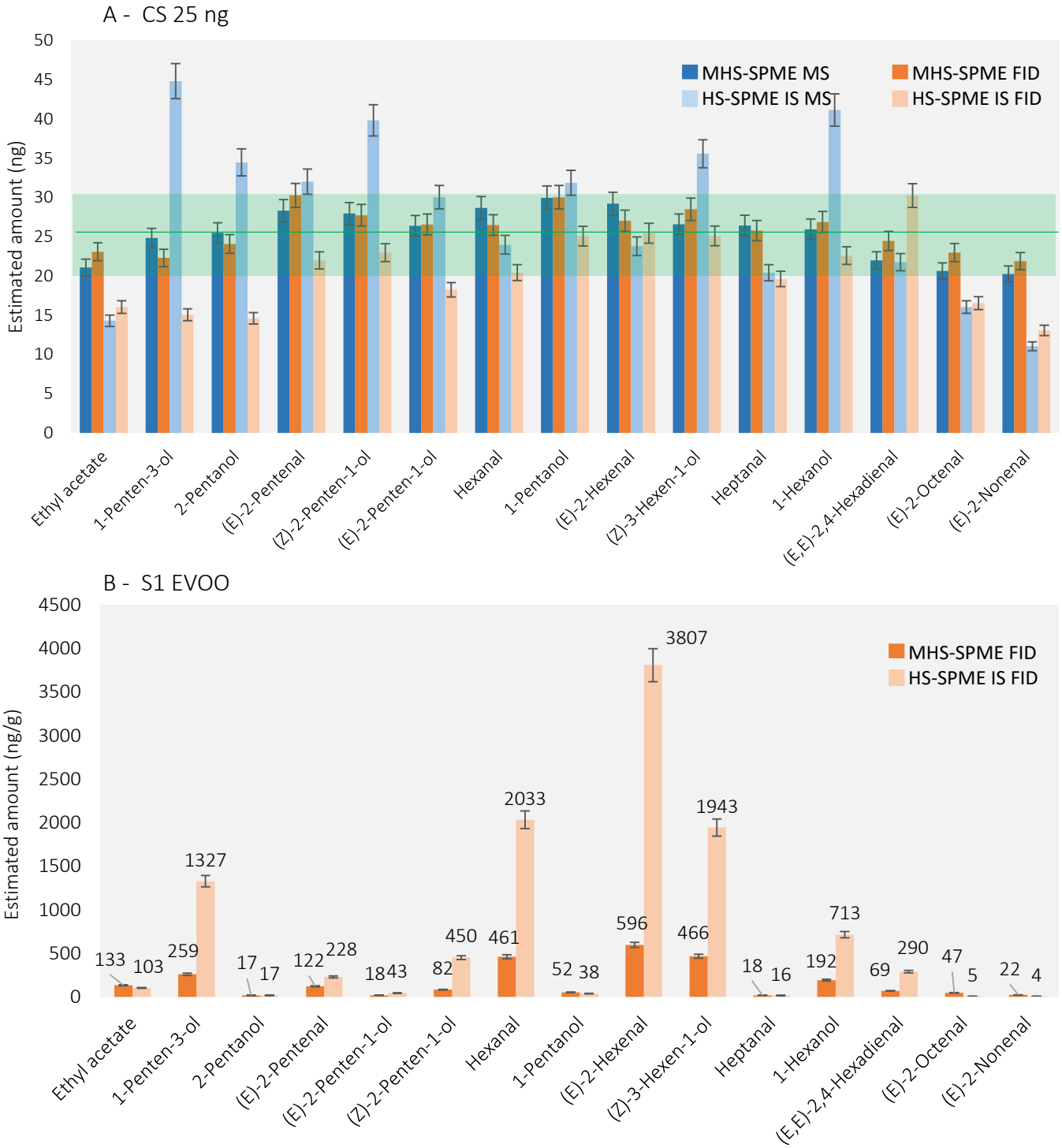

Figure 3: PLS-DA score plots resulting from the model for regional discrimination of samples and based on the UT peaks responses (3A) or quantitated targeted compounds from Table 3 (3B).

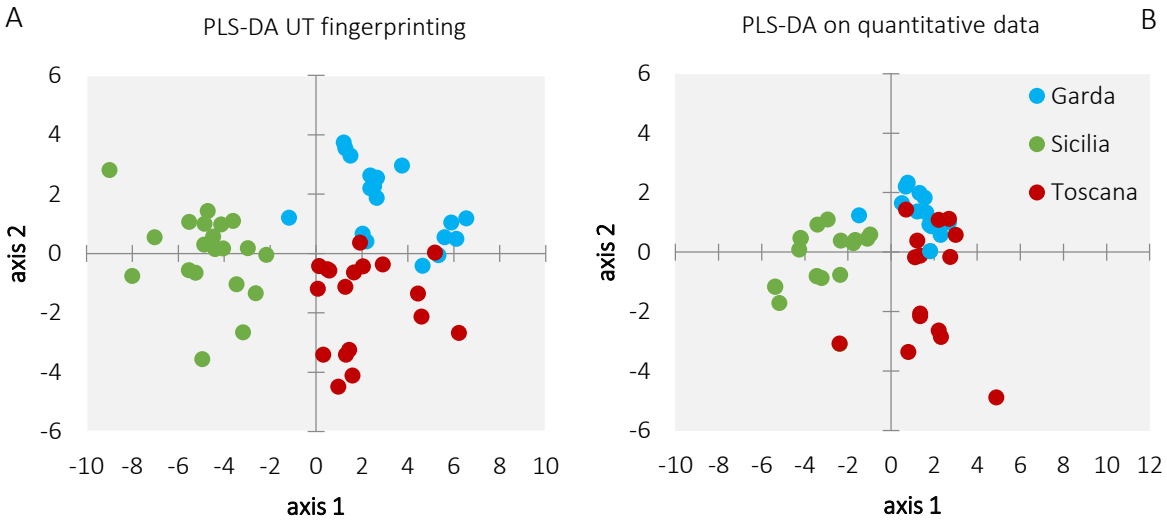

Figure 4: Box-plots illustrating the minimum, maximum, median, and mean quantitative values (red mark) for selected discriminant targeted compounds.

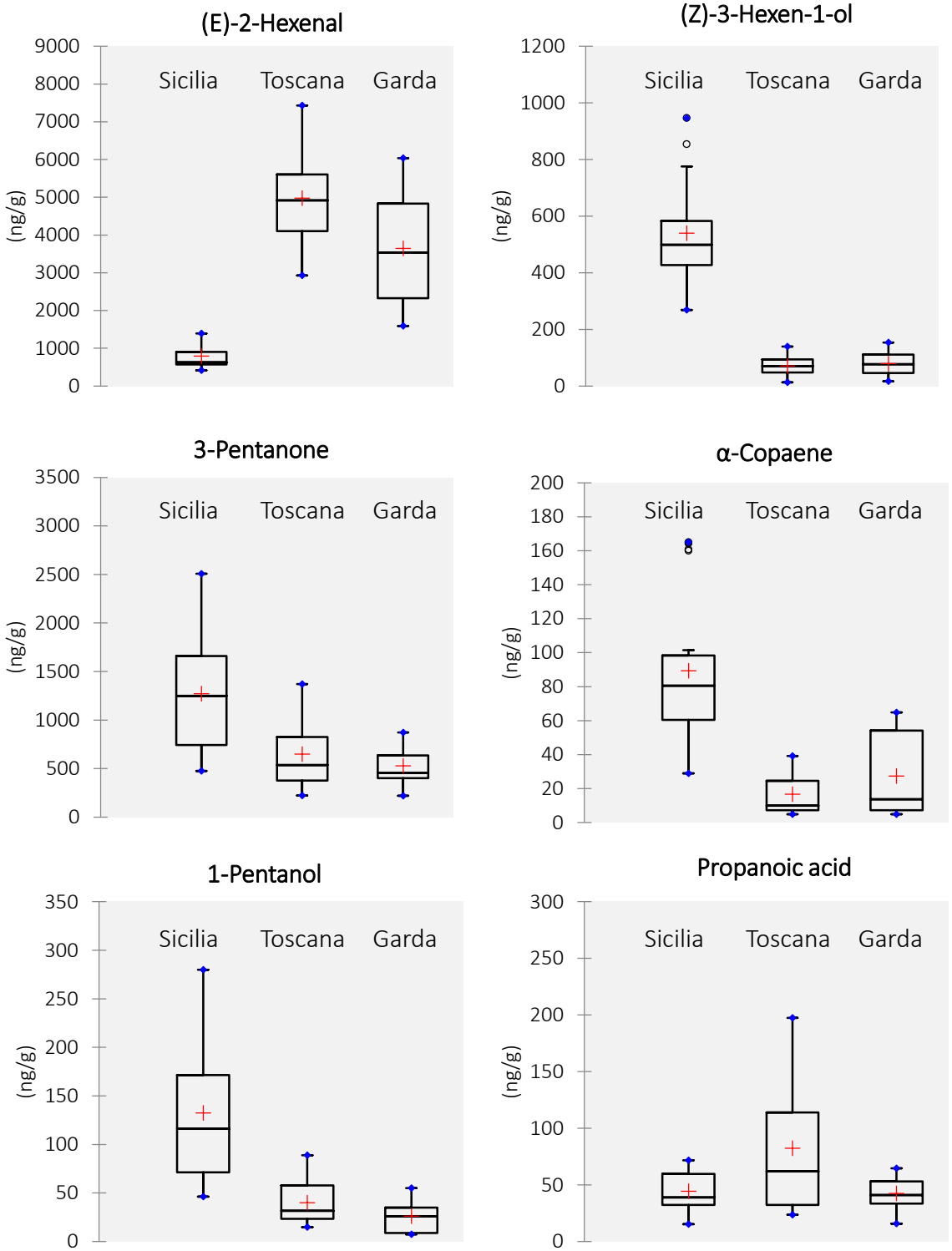

Figure 5: Spider-diagrams showing the EVOOs aroma blueprint and based on calculated OAVs (reported in logarithmic scale). Key-aroma compounds are reported in descending order taking the Garda lake group as reference. Odor qualities are also indicated.

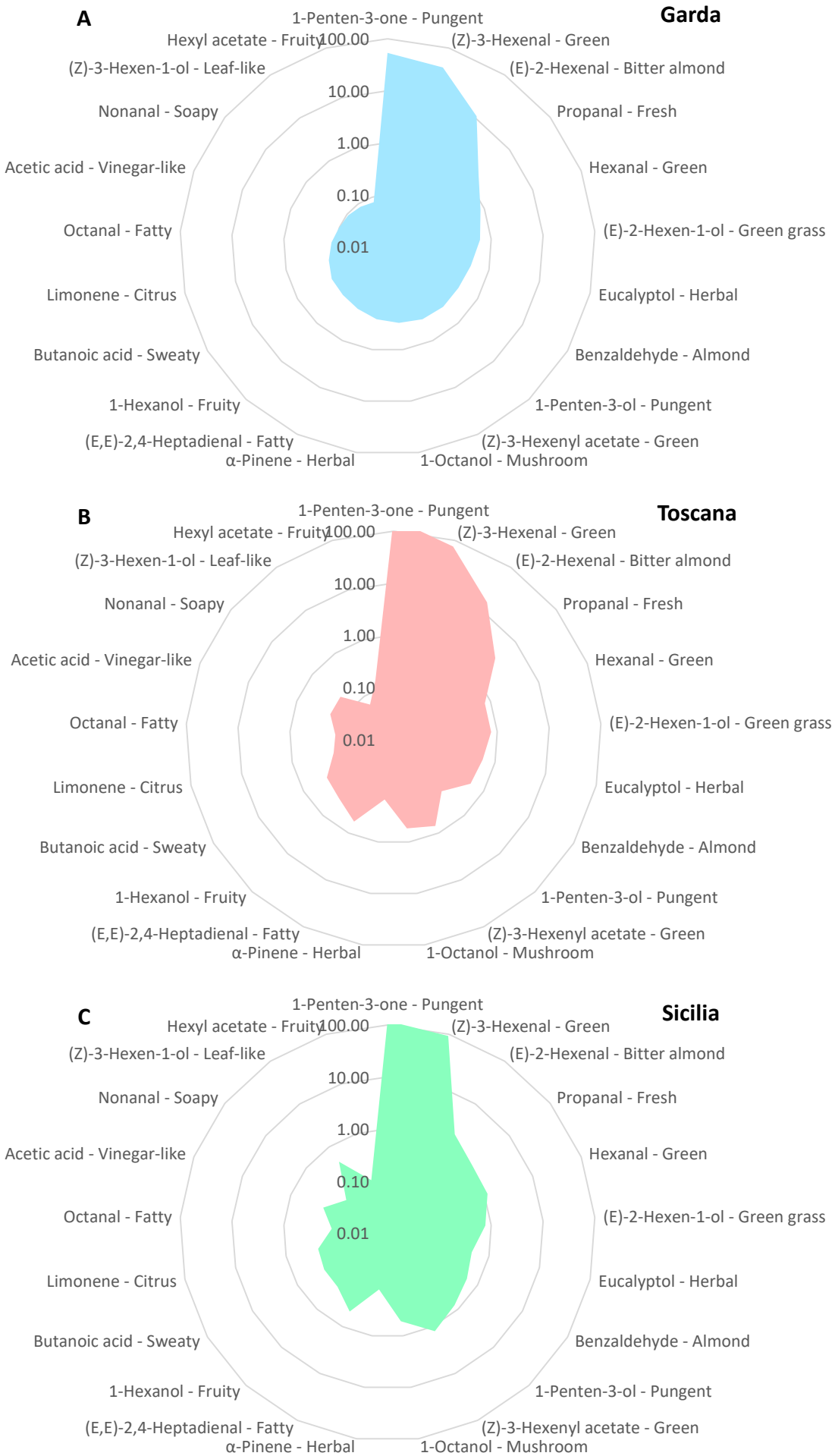

Supplementary material

Delineating the extra-virgin olive oil aroma blueprint by multiple headspace solid phase microextraction and differential-flow modulated comprehensive two-dimensional gas chromatography

Federico Stilo[1], Maria del Pilar Segura Borrego[2], Carlo Bicchi[1], Sonia Battaglino[1], Raquel Maria Callejón Fernadez[2], Maria Lourdes Morales[2], Stephen E. Reichenbach[3,4], James Mc Curry[5], Daniela Peroni[6], Chiara Cordero[1]*

Authors' affiliation:

1. University of Turin, Dipartimento di Scienza e Tecnologia del Farmaco, Turin, Italy
2. Área de Nutrición y Bromatología, Dpto. de Nutrición y Bromatología, Toxicología y Medicina Legal, Facultad de Farmacia, Universidad de Sevilla, Sevilla, Spain
3. Computer Science and Engineering Department, University of Nebraska – Lincoln, Lincoln, NE, USA
4. GC Image, LLC, Lincoln, NE, USA
5. Agilent Technologies, Gas Phase Separations Division, Wilmington DE, USA
6. SRA Intruments SpA, Cernusco sul Naviglio, Milan, Italy

*Corresponding author:

Dr. Chiara Cordero - Dipartimento di Scienza e Tecnologia del Farmaco, Università di Torino, Via Pietro Giuria 9, I-10125 Torino, Italy – e-mail: chiara.cordero@unito.it; phone: +39 011 6707172

Reference solutions and calibration mixtures – schematic diagram

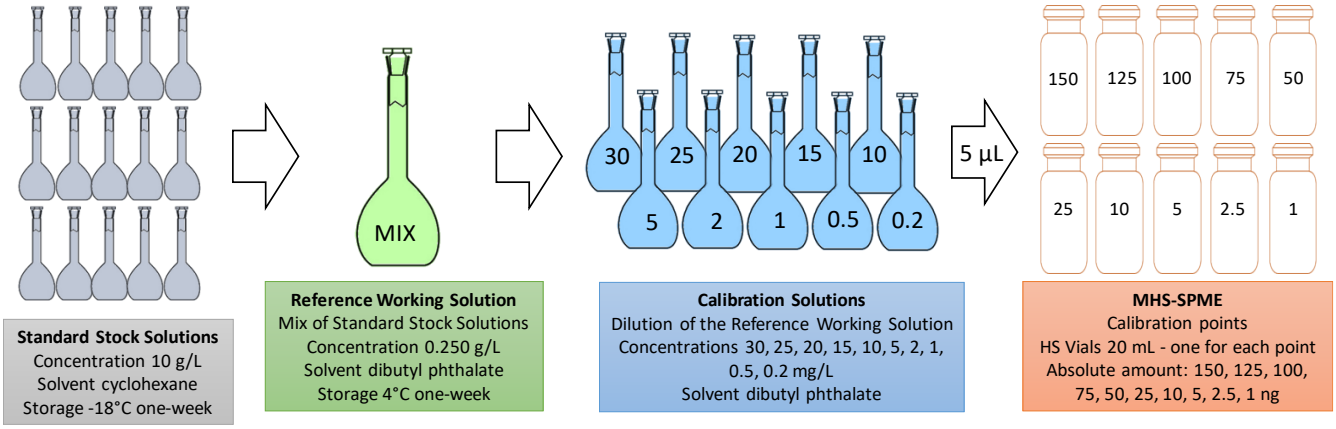

Equations and Procedural steps for Quantification approaches

Response normalization by Internal Standards (ISs) is commonly adopted in gas chromatography. By **Equation 1** quantitative estimations based on ISs relative response for liquid samples/extracts are possible.

Equation 1. $$C_x = \frac{A_x * C_s}{A_s * F}$$

where C_X is the concentration of the compound of interest and A_X is its instrumental response/chromatographic area; C_S and A_S are respectively the concentration and the instrumental response/chromatographic area of the IS; F is the response factor, *i.e.*, the detector relative response of the analyte vs. the IS. Equation 1 does not include any variable compensating and/or accounting for analytes' HS distribution and/or partition/accumulation onto the SPME materials.

Multiple Headspace Extraction (MHE) was introduced by Suzuki *et al.* [1] and McAuliffe [2] for static HS sampling to measure the total amount of the target analyte in an investigated matrix. It was further developed and modeled by Kolb and Ettre [3] and then successfully extended to HS-SPME sampling [4–9]. Principles of operation and fundamental equations are well detailed in reference literature [4–9] and briefly summarized through the fundamental steps.

Step 1. Exhaustive extraction of the targeted analytes, listed in **Table 2** of the manuscript, from the HS of suitable amounts (5µL) of calibration solutions (CSs) and from a selection of representative EVOO samples. Response data from CSs and referring to parallel detection, is adopted to build calibration curves. CSs were prepared within a range of absolute analytes' amounts (1-150 ng) matching concentrations in real-world samples. Response data for targeted analytes in real-world samples (*i.e.*, selected EVOOs) are adopted to verify HS linearity (*i.e.*, absence of saturation phenomena) and estimate decay curve coefficients (β). Headspace linearity is fundamental to verify the linear relationship between the original concentration of the analyte(s) in the sample (C_0) and its concentration in the HS (C_G). The actual linear range, usually included in the concentration interval between 0.1 and 1%, depends on analyte solubility and activity coefficient. Its prediction is challenging and experimental determination is mandatory to achieve reliable results [10–12].

Step 2. Application of the optimized MHS-SPME procedure to the entire sample set. When HS linearity is matched, an analyte's chromatographic response/area (A_S) decreases exponentially with the number of consecutive extractions, while the partition constant (K_{HS}) between the condensed phase and the HS remains constant. The sum of the A_S from each

consecutive extraction step corresponds to the total area or total instrumental response (A_T) for the analyte originally present in the condensed phase, which can be calculated from **Equation 2**:

Equation 2. $$A_T = \sum_{i=1}^{\infty} A_i = A_1 \left(\frac{1}{1 - e^{-q}}\right) = \frac{A_1}{1 - \beta}$$

where A_T is the total estimated area, A_1 is the area resulting from the first extraction, and q is a constant describing the exponential decay of the area with successive extractions. The term q can be obtained by plotting the natural logarithm of chromatographic areas as a function of the number of extraction steps.

The β coefficient is analyte dependent and in general it is constant in samples showing comparable matrix effect. Indicating the extent of the decay across successive extractions, β intrinsically confirms, or not, HS linearity when ≤ 0.95. Moreover, its dependence on K_{HS} offers additional information on matrix behavior and on the release of the target analyte into HS under the applied conditions.

References

[1] M. Suzuki, S. Tsuge, T. Takeuchi, Gas Chromatographic Estimation of Occluded Solvents in Adhesive Tape by Periodic Introduction Method, Anal. Chem. 42 (1970) 1705–1708. doi:10.1021/ac50160a035.

[2] MCAULLIFE C, GC determination of solutes by multiple phase equilibration, Chem. Tech. (1971) 46–51.

[3] B. Kolb, L.S. Ettre, Theory and practice of multiple headspace extraction, Chromatographia. 32 (1991) 505–513. doi:10.1007/BF02327895.

[4] C. Bicchi, M.R. Ruosi, C. Cagliero, C. Cordero, E. Liberto, P. Rubiolo, B. Sgorbini, Quantitative analysis of volatiles from solid matrices of vegetable origin by high concentration capacity headspace techniques: Determination of furan in roasted coffee, J. Chromatogr. A. 1218 (2011) 753–762. doi:10.1016/j.chroma.2010.12.002.

[5] B. Sgorbini, C. Cagliero, E. Liberto, P. Rubiolo, C. Bicchi, C.E.I. Cordero, Strategies for Accurate Quantitation of Volatiles from Foods and Plant-Origin Materials: A Challenging Task, J. Agric. Food Chem. (2019) 1619–1630. doi:10.1021/acs.jafc.8b06601.

[6] B. Sgorbini, C. Bicchi, C. Cagliero, C. Cordero, E. Liberto, P. Rubiolo, Herbs and spices: Characterization and quantitation of biologically-active markers for routine quality control by multiple headspace solid-phase microextraction combined with separative or non-separative analysis, J. Chromatogr. A. 1376 (2015) 9–17. doi:10.1016/j.chroma.2014.12.007.

[7] R. Costa, L. Tedone, S. De Grazia, P. Dugo, L. Mondello, Multiple headspace-solid-phase microextraction: An application to quantification of mushroom volatiles, Anal. Chim. Acta. 770 (2013) 1–6. doi:10.1016/j.aca.2013.01.041.

[8] Ó. Ezquerro, G. Ortiz, B. Pons, M.T. Tena, Determination of benzene, toluene, ethylbenzene and xylenes in soils by multiple headspace solid-phase microextraction, J. Chromatogr. A. 1035 (2004) 17–22. doi:10.1016/j.chroma.2004.02.030.

[9] W.-Q. Xie, Y.-X. Gong, K.-X. Yu, Enhancing the Sensitivity of Full Evaporation Technique Using Multiple Headspace Extraction Analysis, Chromatographia. 80 (2017) 1263–1268. doi:10.1007/s10337-017-3343-x.

[10] J. Pawliszyn, C.F. Ross, Headspace Analysis, in: Compr. Sampl. Sample Prep., Elsevier, 2012: pp. 27–50. doi:10.1016/B978-0-12-381373-2.10036-5.

[11] F. Stilo, E. Liberto, S.E. Reichenbach, Q. Tao, C. Bicchi, C. Cordero, Exploring the extra-virgin olive oil volatilome by adding extra dimensions to comprehensive two-dimensional gas chromatography and time of flight mass spectrometry featuring tandem ionization: validation of ripening markers in headspace linearity conditio, J. AOAC Int. (2020) 1–14. doi:10.1093/jaoacint/qsaa095.

[12] C. Cordero, A. Guglielmetti, B. Sgorbini, C. Bicchi, E. Allegrucci, G. Gobino, L. Baroux, P. Merle, Odorants quantitation in high-quality cocoa by multiple headspace solid phase micro-extraction: Adoption of FID-predicted response factors to extend method capabilities and information potential, Anal. Chim. Acta. 1052 (2019) 190–201. doi:10.1016/J.ACA.2018.11.043.

Supplementary Table 1. List of the 101 target compounds together with their retention times in the two chromatographic dimensions (^1t_R - min, ^2t_R - sec), experimental I^T, odor quality, odor threshold (OT ng/g) in oil, and method of quantification used: (a) compounds quantified through MHS-SPME and calibration curves, (b) compounds quantified by MHS-SPME and FID RRFs.

Compound Name	^1t_R (min)	^2t_R (s)	Exp. I^T	Odor quality	OT (ng/g)	Quantification
Hexane	3.14	0.37	600	-	-	-
1,4-Pentadiene	3.64	0.34	664	-	-	-
Cyclohexane	3.99	0.67	701	-	-	-
2-Methylpentane	4.06	0.44	713	-	-	-
Octane	4.74	0.88	800	Solvent, unpleasant	-	-
Propanal	4.75	0.38	802	Fresh, fruity, malty	9.4[2]	b
Butanal	6.14	0.51	854	Chocolate, pungent	150[1]	-
Ethyl acetate	6.44	0.54	865	Fruity, sweet, winey	940[3]	a
2-Methyl-2-propanol	6.53	0.48	877	Camphor	1000[1]	-
3-Methyl butanal	7.14	0.64	892	Aldehydic, fruity	13[1]	-
Dichloromethane	7.59	0.40	909	-	-	-
Ethanol	7.63	0.34	914	Alcoholic, ethereal	30000[1]	-
3,4-Diethyl-1,5-hexadiene (RS/SR)	8.08	1.33	928	-	-	-
2-Ethylfuran	8.19	0.67	930	Chemical, solvent	8000[1]	-
3,4-Diethyl-1,5-hexadiene (meso)	8.43	1.31	941	-	-	-
3-Pentanone	8.94	0.74	956	Ethereal, acetone	-	b
Pentanal	9.88	0.64	989	Fermented, winey	240[1]	-
(Z)-1-Methoxy-3-hexene	9.94	1.15	991	-	-	-
(5Z)-3-Ethyl-1,5-octadiene	10.09	1.58	996	-	-	-
1-Penten-3-one	10.44	0.61	1007	Pungent, spicy	1.6[2]	b
(5E)-3-Ethyl-1,5-octadiene	10.64	1.55	1012	-	-	-
Toluene	11.09	0.84	1024	Sweet	94000[1]	-
α-Pinene	11.11	1.69	1026	Herbal, woody	274[1]	b
(E)-2-Butenal	11.69	0.61	1039	-	-	-
(E,Z)-3,7-Decadiene	12.69	1.79	1066	-	-	-
2-Methyl-1-propanol	12.74	0.43	1070	Ethereal	1000[1]	-
Hexanal	12.94	0.88	1072	Green-apple, grass	300[2]	a
(E,E)-3,7-Decadiene	13.04	1.79	1075	-	-	-
Camphene	13.11	1.61	1078	Woody, camphoreus	-	b
Undecane	13.59	2.36	1089	-	-	-
2-Pentanol	13.79	0.47	1095	Musty, fermented	380[1]	a
2,4-Dimethyl-3-pentanone	14.74	1.01	1117	Acetone-like	-	-
(E)-2-Pentenal	14.89	0.71	1121	Pungent, apple-like	300[3]	a
β-Pinene	15.30	1.66	1129	Herbal, pine	-	b
(Z)-3-Hexenal	15.39	0.74	1132	Green, grassy	1.7[2]	b
1-Butanol	15.39	0.40	1132	Fermented, fruity	38[1]	-
δ-3-Carene	16.14	1.58	1150	Citrus, pine	-	b
1-Penten-3-ol	16.19	0.40	1151	Pungent, butter	400[3]	a
m-Xylene	16.20	0.72	1151	-	-	-
Heptanal	17.44	0.94	1179	Citrus-like, fatty	500[2]	a
o-Xylene	17.61	0.69	1183	-	-	-
Limonene	17.89	1.55	1190	Citrus, terpenic	250[1]	b
(E)-2-Buten-1-ol	17.90	0.52	1190	-	-	-
Dodecane	18.14	2.49	1195	-	-	-
3-Methyl-1-butanol	18.20	0.34	1197	Fermented, fusel	100[1]	-
Eucalyptol	18.57	1.61	1205	Herbal, minty	15[1]	b
(E)-2-Hexenal	18.94	0.74	1213	Bitter almond, green, fruity	320[2]	a
4-Ethyltoluene	18.94	0.58	1213	-	-	-
Butyl butanoate	19.04	1.25	1216	Fruity, sweet	-	-
1-Pentanol	20.14	0.44	1240	Sweet, pungent	470[3]	a
(E)-β-ocimene	20.44	1.31	1249	-	-	-
Hexyl acetate	21.49	1.04	1271	Fruity	200 [2]	b
p-Cymene	22.05	0.71	1282	Terpenic, fresh	18000[1]	-

Octanal	22.14	0.98	1285	Citrus-like, fatty	140[2]	b
Tridecane	22.69	2.56	1298	-	-	-
(E)-4,8-Dimethylnona-1,3,7-triene	22.94	1.45	1303	-	-	-
(Z)-2-Penten-1-ol	23.04	0.40	1306	Green, almond	250[1]	a
(E)-2-Penten-1-ol	23.39	0.40	1314	Plastic, rubber	250[1]	a
(Z)-3-Hexenyl acetate	23.54	0.94	1317	Sweet	200[2]	b
(E)-2-Heptenal	23.69	0.84	1321	Green, fatty	1200[2]	b
6-Methyl-5-hepten-2-one	23.88	0.93	1327	Pungent, green	1000[1]	b
1-Hexanol	24.79	0.51	1346	Fruity, banana, soft	400[3]	a
(Z)-3-Hexen-1-ol	26.24	0.44	1379	Banana, fresh, grass	1100[1]	a
Nonanal	26.84	1.08	1393	Citrus-like, soapy	610[2]	b
(E,Z)-2,4-Hexadienal	26.94	0.57	1395	Green	-	-
(E,E)-2,4-Hexadienal	27.14	0.57	1400	Green	270[1]	a
3-Methyl-4-heptanone	27.18	0.88	1401	-	-	-
(E)-2-Hexen-1-ol	27.19	0.40	1401	Green grass, leaves	5000[1]	b
Acetic acid	27.56	0.22	1409	Sour, vinegary	500[1]	b
α-Thujone	28.09	1.11	1422	Thujonic	-	-
(E)-2-Octenal	28.34	0.81	1428	Fatty, nutty	120[2]	a
β-Thujone	28.94	1.11	1442	Thujonic	-	-
1-Heptanol	29.35	0.53	1451	Herb	10[1]	-
(E,E)-2,4-Heptadienal	29.84	0.64	1464	Fatty, green, oily	30[2]	b
α-Copaene	30.99	2.22	1491	Woody	-	b
Decanal	31.22	1.17	1499	Penetrating, sweet, waxy	650[1]	-
Benzaldehyde	32.39	0.61	1524	Almond, burnt sugar	60[1]	b
(E)-2-Nonenal	32.79	0.84	1534	Fatty, green, soapy	140[2]	a
Propanoic acid	32.99	0.24	1539	Acidic, pungent	720[1]	b
1-Octanol	33.49	0.54	1551	Nut, mushroom	27[1]	b
Butanoic acid	34.35	0.25	1578	Cheesy, sour	34[1]	b
Undecanal	35.32	1.27	1592	Sweet, fatty, floral-citrus	6800[1]	-
Butyrolactone	36.61	0.47	1613	Creamy, milky	-	b
(E)-2-Decenal	37.03	0.87	1632	Waxy, fatty, earthy	10[1]	-
Methyl-2-octynoate	37.49	0.88	1653	-	-	-
1-Nonanol	37.56	0.56	1655	Fresh, clean, floral	280[1]	-
Y-Hexalactone	38.10	0.52	1670	Tonka, creamy	-	b
Dodecanal	39.40	1.36	1693	Soapy, fatty, aldehydic	3000[1]	-
α-Muurolene	40.19	1.75	1724	-	-	-
Pentanoic acid	40.74	0.25	1739	Cheesy, acidic	600[1]	-
α-Farnesene	41.08	1.38	1753	Woody, green	-	b
Butyl benzoate	43.24	0.24	1807	Balsamic, amber	-	-
1,4-Cyclohex-2-enedione	44.19	0.51	1834	-	-	-
Hexanoic acid	44.64	0.26	1846	Goat-like, sweaty	700[1]	-
Phenylethyl alcohol	45.20	0.38	1863	Floral, sweet	210[1]	-
Isobutyl benzoate	45.29	0.94	1865	Balsamic, fruity	-	-
Benzyl alcohol	45.54	0.34	1872	Sweet, fruity	59000[1]	-
Heptanoic acid	48.49	0.26	1962	Cheesy, waxy	100[1]	-
Phenol	49.94	0.24	1999	-	-	-
Phthalide	60.84	0.51	2353	Coumaric, sweet	-	-
Dibutyl phthalate (IS dilution solvent)	70.29	1.04	2630	-	-	-

[1] L.J. Van Gemert, Odour Thresholds - Compilations of odour thresholds values in air, water and other media, 2011.
[2] A. Neugebauer, M. Granvogl, P. Schieberle, Characterization of the Key Odorants in High Quality Extra Virgin Olive Oils and Certified Off-Flavor Oils to Elucidate Aroma Compounds Causing a Rancid Off-Flavor, J. Agric. Food Chem. (2020) acs.jafc.0c01674. https://doi.org/10.1021/acs.jafc.0c01674.
[3] G. Luna, M.T. Morales, R. Aparicio, Characterisation of 39 varietal virgin olive oils by their volatile compositions, Food Chem. 98 (2006) 243–252. https://doi.org/10.1016/j.foodchem.2005.05.069

Supplementary Figure 1. Production regions, over Italian territory, for selected EVOO samples.

Supplementary Table 2. List of the 184 untargeted and targeted peak features together with their retention times in the two chromatographic dimensions (^1t_R - min, ^2t_R - sec), experimental I^T, and EI-MS spectrum.

Provided as a Microsoft Excel file.

Supplementary Table 3. Results from quantitative analysis of fifteen targeted analytes subjected to external calibration by MHS-SPME and MS/FID or HS-SPME IS normalization. Accuracy is shown for calibration solutions (CS at 1-10-25 and 100 ng absolute amount) and for real samples analyzed by the quantitative approaches. Results are provided together with ±standard deviation (SD) calculated over analytical replicates (n=3) acquired over two-weeks.

Targeted analyte	Accuracy MHS-SPME FID *vs.* MS (RE%)				MHS-SPME FID quantitation in EVOO samples (ng/g)											
	CS1	CS10	CS25	CS100	S1	±SD	S8	±SD	T3	±SD	T10	±SD	G6	±SD	G12	±SD
Ethyl acetate	10	8	9	7	133	11	558	50	122	11	279	25	266	18	218	29
Hexanal	7	8	8	6	461	45	358	35	251	25	148	15	159	33	306	23
2-Pentanol	5	6	6	7	17	2	17	2	13	1	13	1	14	1	16	1
(E)-2-Pentenal	6	7	6	5	122	4	174	5	200	6	78	2	59	2	70	2
1-Penten-3-ol	9	11	11	9	259	19	368	27	92	7	172	13	59	12	221	10
Heptanal	3	2	3	3	18	1	17	1	12	1	15	1	14	1	16	1
(E)-2-Hexenal	7	6	8	10	1981	85	638	27	3144	135	5603	241	3619	218	3059	212
1-Pentanol	3	3	3	4	52	2	126	5	9	1	26	1	27	1	34	1
(Z)-2-Penten-1-ol	1	3	4	2	82	5	209	13	62	4	157	10	125	8	170	8
(E)-2-Penten-1-ol	2	1	3	5	18	1	46	1	49	1	27	1	27	1	36	1
1-Hexanol	3	2	3	4	192	7	73	3	50	2	103	4	120	6	121	7
(Z)-(3)-Hexen-1-ol	7	8	7	6	466	17	419	15	66	2	94	3	88	3	182	4
(E,E)-2,4-Hexadienal	11	9	10	11	69	4	43	2	70	4	32	2	28	1	22	1
(E)-2-Octenal	11	11	10	8	47	4	43	5	36	3	40	3	39	4	41	3
(E)-2-Nonenal	12	12	15	15	22	1	43	1	17	1	20	1	39	1	41	1

Targeted analyte	HS-SPME IS quantitation in EVOO samples (ng/g)											
	S1	±SD	S8	±SD	T3	±SD	T10	±SD	G6	±SD	G12	±SD
Ethyl acetate	103	9	535	48	285	25	210	19	159	14	306	27
Hexanal	2083	204	1500	147	4265	418	760	75	1458	143	1160	114
2-Pentanol	17	2	14	1	17	2	5	1	5	1	6	1
(E)-2-Pentenal	228	7	294	9	1218	35	108	3	117	3	133	4
1-Penten-3-ol	1327	97	1684	123	1434	105	662	48	737	54	649	47
Heptanal	16	1	12	1	8	1	6	1	10	1	10	1
(E)-2-Hexenal	3814	164	3609	155	6147	264	8228	354	9431	406	9193	395
1-Pentanol	38	2	79	3	23	1	14	1	21	1	21	1
(Z)-2-Penten-1-ol	450	28	1043	66	1072	68	669	42	634	40	650	41
(E)-2-Penten-1-ol	43	1	142	3	549	12	62	1	72	2	86	2
1-Hexanol	713	27	242	9	605	23	294	11	498	19	596	23
(Z)-(3)-Hexen-1-ol	1943	70	1555	56	1190	43	369	13	437	16	461	17
(E,E)-2,4-Hexadienal	290	15	143	7	941	48	83	4	82	4	36	2
(E)-2-Octenal	5	1	7	1	9	1	3	1	4	1	3	1
(E)-2-Nonenal	4	1	7	0	6	1	5	1	8	1	4	1

Supplementary Table 4. Results from quantitative analysis of 42 targeted analytes obtained by MHS-SPME and FID RRFs. Data expressed in ng/g, refers to the mean of three analytical replicates acquired over two weeks of method application; uncertainty is reported as ±standard deviation (SD).

Provided as a Microsoft Excel file.